NASA Technical Paper 1063

Effects of Continuous and Cyclic Thermal Exposures on Boron- and Borsic-Reinforced 6061 Aluminum Composites

George C. Olsen and Stephen S. Tompkins

NOVEMBER 1977

NASA

NASA Technical Paper 1063

Effects of Continuous and Cyclic Thermal Exposures on Boron- and Borsic-Reinforced 6061 Aluminum Composites

George C. Olsen and Stephen S. Tompkins
Langley Research Center
Hampton, Virginia

National Aeronautics
and Space Administration

**Scientific and Technical
Information Office**

1977

SUMMARY

Boron-aluminum (B/Al) and Borsic-aluminum (Bsc/Al) composites were continuously exposed at 728 K for up to 240 hours and at 783 K for up to 12 hours and cyclically exposed between 293 K and 728 K for up to 6000 cycles. Room-temperature tensile strengths were measured and the specimens were metallographically examined. Scanning-electron-microscope energy dispersive analysis of X-rays and an X-ray diffraction technique were employed to determine the reaction products at the fiber/matrix interface.

Formation of an AlB_2 reaction layer has previously been associated with the degradation of boron-aluminum composites. The data of this report suggest that in addition to AlB_2 formation, magnesium in the 6061 aluminum matrix diffused to the reaction layer and formed $(Al,Mg)B_2$. Formation of $(Al,Mg)B_2$ could weaken the matrix and embrittle the reaction layer. Continuous thermal exposure degraded the strength of the B/Al specimens, but the noncumulative fracture mode, indicative of high-strength interfaces, did not change. The strength degradation was attributed to crack initiation in the brittle reaction layer causing stress concentrations on the fibers. Continuous exposure did not alter the strength of the Bsc/Al specimens. Cyclic thermal exposure degraded the strength of both materials, but the strength of Bsc/Al specimens was degraded to a lesser extent than the B/Al specimens. The cyclic exposure specimens showed transition toward a cumulative fracture mode, characteristic of low interfacial strength. The lower interfacial strengths were attributed to weakened planes caused by reversing stress fields induced by differential thermal expansion. Cyclic exposure degraded the strength of the B/Al specimens more than continuous exposure.

INTRODUCTION

Composites of aluminum alloy matrix reinforced with boron fibers are subject to degradation of mechanical properties when continuously or cyclically exposed to elevated temperatures. (See refs. 1 to 6.) The degradation has been attributed to formation of a reaction layer of aluminum diboride (AlB_2) which either weakens the interfacial bond or introduces stress concentrations in the fiber (ref. 2). The rate of degradation of boron-aluminum composites has been observed to vary widely depending upon the aluminum alloy used for the matrix (refs. 4 and 6). This variation has not been explained and suggests that the degradation mechanism is more complex than anticipated and may involve alloying constituents of the matrix.

An experimental investigation was conducted to determine what mechanisms cause the degradation of strength in these aluminum matrix composites. This report presents effects of continuous and cyclic exposure to elevated temperatures on 6061 aluminum matrix composites reinforced with boron and silicon-carbide-coated boron fibers.

ABBREVIATIONS

B/Al	boron-aluminum composites
Bsc/Al	Borsic-aluminum composites
EDAX	energy dispersive analysis of X-rays
SEM	scanning electron microscopy
UTS	ultimate tensile strength

MATERIALS, EXPOSURE ENVIRONMENT, AND ANALYSES

Materials

Two fiber-reinforced 6061 aluminum matrix composite materials were investigated. One (B/Al) was reinforced with 0.142-mm-diameter boron fibers, and the other (Bsc/Al) was reinforced with 0.145-mm-diameter silicon-carbide-coated boron (Borsic) fibers. The materials were fabricated in 30.5-cm by 50.8-cm panels with a 6-ply unidirectional lay-up. The panels were consolidated by diffusion bonding. The diffusion bonding parameters for the B/Al panels were a pressure of 31 MPa and a temperature of 800 to 805 K for 30 minutes and for the Bsc/Al panels were 31 MPa and 820 to 825 K for 30 minutes. The resulting fiber volume fractions were nominally 0.49, and panel thicknesses were nominally 0.106 cm for the B/Al panels and 0.110 cm for the Bsc/Al panels. No flaws were detected in the finished panels by either ultrasonic or X-ray examination.

Tensile test specimens cut from the panels were 15.24 cm long by 1.27 cm wide with the fibers oriented longitudinally. A schematic diagram of a specimen with adhesively bonded fiber glass gripping tabs for tensile testing is shown in figure 1.

Thermal Exposure Environments

The specimens were either continuously exposed to elevated temperatures or cycled between an elevated temperature and room temperature. The exposure temperatures considered are well above any anticipated use temperature. These high temperatures were selected to accelerate the degradation mechanisms and are typical of many of the exposure temperatures reported in the literature.

Continuous exposure.- Thermal exposures were conducted in a bath of fluidized aluminum oxide particles. The particles were contained in a vertical cylinder, 16.5 cm in diameter and 40.6 cm high, and were fluidized by a vertical flow of dry, filtered, compressed air. The air pressure and flow rate could be adjusted to maintain proper fluidization. Four electric heaters at the inside perimeter of the cylinder maintained bath temperatures of up to 867 K to $\pm$1 percent. The high thermal conductivity and turbulent mixing in the bath resulted in spatial temperature deviations of less than $\pm$0.5 percent and heat-transfer rates at solid surfaces approaching those in liquids.

Continuous exposures were conducted at two temperatures for the following times:

(1) At 728 K for 80, 120, 160, 200, and 240 hours

(2) At 783 K for 5, 8, 10, and 12 hours

Three specimens of each composite material were exposed at each temperature-time condition. One additional specimen of each material was exposed at 783 K for 170 hours to produce a thick reaction layer for metallographic analysis.

The fluidized bath was heated to the exposure temperature and allowed to stabilize before the specimens, suspended unrestrained in a stainless steel wire cage, were submerged in it. The temperature of the bath was continuously measured by a chromel-alumel thermocouple suspended in the bath. As specimens completed their exposure times, they were removed from the bath and allowed to cool in air to room temperature.

Cyclic exposure.- The elevated temperature segment of the cycle was conducted in a fluidized bath like the one used for the continuous exposures. The lower temperature segment of the cycle was conducted in another fluidized bath modified by installing a helically wound copper cooling coil at the inside perimeter of the container. A laboratory cooling unit continuously circulated a chilled ethylene glycol solution through the coil to remove the heat added by the specimens and maintain the lower temperature in the bath.

The specimens were transferred from bath to bath by the mechanism shown in figure 2. Each full cycle was recorded by an automatic counter. A timer controlled the time the rack remained in each bath.

Cyclic thermal exposures were conducted between 293 K and 728 K. Specimens of each composite material were exposed to the cycling environment for each of the following number of cycles: 1000, 2057, and 6000 cycles. A typical temperature cycle for a specimen instrumented with a chromel-alumel thermocouple is shown in figure 3. A complete cycle lasted 3.4 minutes with approximately 1 minute in the 293 K bath and approximately 1 minute in the 728 K bath. The balance of the time was required to transport the specimens between the two baths. During transport, the specimens were exposed to room-temperature air.

The fluidized baths were brought to the exposure temperatures and allowed to stabilize before beginning the exposures. The temperature of a calibration specimen mounted on the rack was continuously measured by an attached chromel-alumel thermocouple connected to a strip-chart recorder.

Tensile Tests

Room-temperature tensile strength tests were conducted on the thermally exposed specimens and on a control group of unexposed specimens. The specimens were instrumented with strain gages and tested in a 0.53-MN hydraulic testing machine. Each specimen was centered in the testing machine wedge grips, and a small load was applied to set the grips in the gripping tabs. The machine load

output and the strain gage output were connected to an X-Y plotter to provide a load/strain curve for the specimen. Load was applied to the specimen at a constant strain rate of 0.01 (cm/cm)/min to failure.

Metallographic Analyses

Representative specimens from each exposure condition and an unexposed specimen were selected for the following metallographic analyses:

(1) Fracture surfaces were examined with scanning electron microscopy (SEM).

(2) Elemental constituents in the matrix and reaction layer were determined from the fracture surfaces using SEM energy dispersive analysis of X-rays (EDAX).

(3) Polished and etched cross sections of the specimens were examined with optical microscopy.

(4) The fiber strength distribution for approximately 40 fibers from each specimen was determined by the fiber bend method described in reference 7. The fibers were bent around the successively smaller mandrels of the test fixture shown in figure 4 until they failed. The fibers (approximately 5 cm long) were obtained from specimen sections by chemically removing the aluminum matrix in a heated solution of NaOH.

(5) Reaction layer morphology on chemically removed fibers was examined. The fibers were prepared by etching one end with Murakami's reagent which detached the reaction layer by etching away the boron fiber beneath it. The interface between the etched and unetched regions was then examined with SEM.

(6) Chemical compounds present in the reaction layer were determined by analyzing the X-ray diffraction pattern of a powder sample. The powder sample was prepared from chemically removed fibers. The reaction products were removed from the fibers by ultrasonic cleaning in a distilled water bath. The residue from the cleaning process was dried and sieved through a 200 mesh screen to form the powder sample. A goniometer and diffractometer were used to obtain the X-ray diffraction patterns.

RESULTS AND DISCUSSION

Typical tensile stress-strain curves for exposed and unexposed specimens are shown in figure 5. The presence of two linear regions, called stage I and stage II, is typical behavior for this type composite and is discussed in reference 8, pages 432-433. The room-temperature ultimate tensile strength (UTS) and stage II modulus for each continuous thermal exposure specimen and for each cyclic thermal exposure specimen are listed in tables I and II, respectively. Neither continuous nor cyclic exposure had any apparent effect on the room-temperature modulus. The mean stage II modulus was 241 GPa with a standard

deviation of 8 GPa for the B/Al specimens and 246 GPa with a standard deviation of 4 GPa for the Bsc/Al specimens.

Continuous Exposure Specimens

Tensile strength and fracture mode.- The mean value and standard deviation of the UTS as a function of continuous exposure time for both B/Al and Bsc/Al are shown in figure 6 for exposure at 728 K and 783 K. Curves have been faired through each set of data. The B/Al UTS decreased in a nearly linear manner as exposure time at 728 K increased (fig. 6(a)). Exposure for 240 hours resulted in 29 percent less strength. The B/Al UTS as a function of continuous exposure time at 783 K decreased in a nonlinear manner (fig. 6(b)). The Bsc/Al strength was not significantly affected by continuous exposure at either temperature. However, much more scatter was present in the Bsc/Al data.

Typical fracture profiles of the B/Al and Bsc/Al specimens are shown in figures 7 and 8, respectively, and SEM fractographs of these specimens are shown in figures 9 and 10. The fracture profiles and surface morphology of these specimens show no indication of a change in fracture mode as a result of continuous thermal exposure. All failures of the continuous exposure specimens are characterized by ductile necking fracture of the matrix and fragmented brittle fracture of the fiber, with no fiber pullout (figs. 9 and 10). Fractures of this type are termed noncumulative mode fractures (ref. 9) and indicate well-consolidated materials with high-strength interfaces.

Higher magnification SEM fractographs and EDAX spectra for elemental analysis of the material in the matrix and at the fiber/matrix interface are shown in figure 11. The EDAX spectra for the unexposed specimen (fig. 11(a)) show that initially the matrix and the material at the interface are similar in composition. The low-concentration alloying constituents in the 6061 aluminum matrix do not appear in the spectra at this scale. After exposure at 728 K for 120 hours (fig. 11(b)) and 240 hours (fig. 11(c)), the concentration of magnesium at the interface was detectable at this scale. This indicates that some of the magnesium that was initially dispersed in the 6061 aluminum matrix had diffused to the interface.

Fiber/matrix interface and fiber strength.- Cross sections from the specimens were polished and etched with Keller's reagent, which deeply etched the reaction layer. When these specimens are viewed with an optical microscope focused on the plane of the reaction-layer/matrix interface, the morphology of this interface becomes visible. Because of the surface relief caused by the polishing process, the entire reaction layer cannot be brought into focus simultaneously, and as a result, the apparent thickness of the reaction layer may be misleading. Photomicrographs of the reaction-layer/matrix interface of unexposed B/Al specimens and specimens continuously exposed at 728 K and 783 K are shown in figures 12 and 13, respectively. These figures show what appears to be development of acicular growth at the fiber/matrix interface, similar to that reported in reference 10. The unexposed specimens (figs. 12(a) and 13(a)) show little or no acicular growth developed during the fabrication process. Exposure to the elevated temperatures caused the acicular growth to develop

(figs. 12(b) and 13(b)). The growth was more dense for longer exposure time (figs. 12(c) and 13(c)).

The reaction layer is more distinctly seen on fibers which have been chemically removed from the matrix and then partially etched with Murakami's reagent. These fibers, from an unexposed specimen and from specimens continuously exposed at 728 K and 783 K, are shown in figure 14. The light, discontinuous initial layer on the unexposed specimen is apparent in figure 14(a). Thicker, continuous layers formed during the continuous exposures are shown in figures 14(c), (d), and (e). A fiber from a specimen exposed 170 hours at 783 K to accentuate the reaction layer is shown in figure 14(f). The fluffy texture of the reaction layer may be attributed to the acicular growth.

X-ray diffraction patterns from a powder sample of the reaction layer contained only two peaks, both of low intensity. One of these corresponded to the major peak for aluminum diboride (AlB_2) and the other corresponded to the major peak for magnesium diboride (MgB_2). The intensity of the secondary peaks for these compounds are only 40 percent and 34 percent of the amplitude of their major peaks and could have been masked by the background pattern. Neither of the peaks found corresponded to any other species. This was not considered a conclusive identification of the reaction products; however, AlB_2 has been identified as a reaction product in a similar specimen analyzed with electron diffraction techniques (ref. 10), and a higher concentration of magnesium was found at the fiber/matrix interface than in the matrix (fig. 11(c)).

These data suggest that the following degradation mechanism may occur. Aluminum and boron may react at the reaction-product/matrix interface to form AlB_2. Available magnesium may preferentially substitute for the aluminum in the reaction and form $(Al,Mg)B_2$ (both AlB_2 and MgB_2 have hexagonal crystal structures). Such a reaction could lower the magnesium concentration in the matrix at the interface and result in a net flux of magnesium from the matrix to the interface.

The result of this mechanism could be twofold. First, the lowered concentration of magnesium (a strengthening agent) in the 6061 aluminum matrix could weaken the matrix material. Secondly, the substitution of magnesium, 11 percent larger in atomic radius than aluminum, into the crystal structure of the reaction layer could embrittle the structure by distorting the lattice.

Polished and etched cross sections of Bsc/Al specimens continuously exposed at 728 K and 783 K are shown in figures 15 and 16, respectively. Unlike the B/Al specimens (figs. 12 and 13), these Bsc/Al specimens had only small patchy sites of acicular growth. This patchy formation is better seen on the fibers partially etched with Murakami's reagent, shown in figure 17. Two photomicrographs of each fiber are shown, one of the unetched end and the other of the etched end. The silicon carbide coating on the fibers apparently retarded the reactions between the fiber and the matrix. However, patches of reaction products formed where the coating was not sufficiently thick.

Fiber strength distributions for various exposure times at 728 K and 783 K are shown in figure 18 for B/Al specimens and in figure 19 for Bsc/Al specimens. The boron fiber strength decreased with the increased exposure time in both

cases, as evidenced by the leftward shift of the distributions. Note, however, that the full amount of shift is not shown because the test fixture used was not capable of measuring strengths greater than 3.74 GPa and a large number of fibers in the unexposed specimens showed higher strengths. The Borsic fibers showed no change in strength with increased exposure time.

Failure mechanism.- Collectively, these data suggest that the failure mechanism for the B/Al continuous thermal exposure specimens could be crack initiation in the reaction layer causing stress concentrations on the surface of the fiber and fiber failure at relatively low stresses. This conclusion is supported by the type and consistency of the fracture mode which indicates that the interface shear strength was adequate to transfer the load, and by the shift in the fiber strength distributions which indicates that the degradation was in the reaction-products/fiber system.

The strengths of the Bsc/Al composite and the Borsic fibers were apparently not changed by continuous thermal exposure. This indicates that although patches of reaction products were found, not enough formed to degrade the strength.

Cyclic Exposure Specimens

Tensile strength and fracture modes.- The mean value and standard deviation of the UTS as a function of the number of cycles between 293 K and 728 K for both B/Al and Bsc/Al are shown in figure 20. Curves have been faired through each set of data. The UTS for both materials degraded in a nonlinear manner as the number of cycles became larger. Exposure to 6000 cycles resulted in a 34 percent loss of strength for B/Al and an 18 percent loss of strength for Bsc/Al. Thermal cycling had no apparent effect on the room-temperature modulus of either material.

Typical fracture profiles of B/Al and Bsc/Al specimens are shown in figures 21 and 22, and SEM fractographs of these specimens are shown in figures 23 and 24. The fracture profiles and surface morphology of these specimens show that the fracture mode changes with cyclic thermal exposure. The unexposed B/Al specimen (fig. 23(a)) failed in the noncumulative mode seen in the continuous thermal exposure specimens. The thermally cycled B/Al specimens (figs. 23(b), (c), and (d)), however, failed in a mixed fracture mode as transition from the noncumulative mode to a cumulative mode occurred. The cumulative mode (ref. 9) is characterized by axial shear-step failures in the matrix, nonfragmenting fracture of the fibers, and fiber pullout from the matrix. This type of fracture mode is indicative of poorly bonded materials and weak interfacial strength. The Bsc/Al specimens (fig. 24) had the same shift in fracture mode, but to a lesser extent.

SEM fractographs at higher magnifications and EDAX spectra for elemental analysis of the material in the matrix and at the fiber/matrix interface are shown in figure 25 for the 6000-cycle specimen. The EDAX spectra from this specimen show that the concentration of magnesium at the interface was greater after exposure than before. This implies that the reaction layer in the cyclic

exposure specimens may be formed by the same mechanism that was discussed for the continuous exposure specimens.

Fiber/matrix interface and fiber strength.- A cross section from a 6000-cycle B/Al specimen was polished and etched. A photomicrograph of the cross section taken in an optical microscope is shown in figure 26. The interface between the reaction layer and the matrix of this specimen appears smooth and does not have the acicular growth developed in the continuous exposure specimens (figs. 12 and 13).

The reaction layer is more distinctly seen on boron fibers partially etched with Murakami's reagent (fig. 27). The reaction layer in the 6000-cycle specimen (fig. 27(d)) might be expected to be similar to that in the 80-hour continuous exposure specimen (fig. 14(b)). However, it does not have the same fluffy texture attributed to the acicular growth.

Fibers from the cycled Bsc/Al specimens are shown in figure 28. As before, two photomicrographs for each fiber are presented, one of the unetched end and the other of the etched end. These fibers show reaction layers similar to those on the continuous exposure test fibers (fig. 17); the silicon carbide coating on the fiber apparently retarded the reactions between the fiber and the matrix. However, patches of reaction products were formed where the coating was not sufficiently thick.

Fiber strength distributions as a function of the number of exposure cycles for both the B/Al and Bsc/Al specimens are shown in figure 29. In contrast to the continuously exposed boron fibers (fig. 18), the thermally cycled boron fibers showed no degradation in strength. Thermal cycling did not degrade the strength of the Borsic fibers.

Failure mechanism.- Collectively, these data suggest that the failure mechanism for the B/Al and Bsc/Al thermally cycled specimens could be the result of degradation of interfacial strength. The reversing stress field at the interface, induced by differences in thermal expansion, could weaken the mechanical bond between the matrix and fiber with each reversal. In the B/Al specimens, additional weakening between the reaction products and the matrix could be caused by the reversing stress field. This stress field could shear off the tips of the acicular growth and create another weakened interface. These conclusions are supported by the transition in fracture mode which indicates an interfacial strength not adequate to transfer the load, by the absence of acicular growth (fig. 27), and by the consistent fiber strength distributions which indicate that failure was not initiated in the reaction-products/fiber system.

CONCLUSIONS

Boron-aluminum (B/Al) and Borsic-aluminum (Bsc/Al) composites have been subjected to continuous exposure at 728 K for up to 240 hours and at 783 K for up to 12 hours and to cyclic exposure from room temperature to 728 K for up to 6000 cycles. The room-temperature tensile strengths were measured and the specimens were metallographically analyzed. Scanning-electron-microscope energy dispersive analysis of X-rays and an X-ray diffraction technique were

employed to determine reaction products at the fiber/matrix interface. The conclusions of the investigation are as follows:

1. Exposure to continuous or cyclic elevated temperatures caused magnesium in the 6061 aluminum matrix to diffuse to the reaction layer. Data suggest that while aluminum and boron react to form AlB_2, available magnesium may preferentially substitute for aluminum in the reaction and form a complex compound, $(Al,Mg)B_2$. This mechanism could result in a weaker matrix and an embrittled reaction layer.

2. Continuous thermal exposure significantly degraded the strength of the B/Al composites but did not alter the modulus or the mode of fracture. The failure mechanism for these specimens appeared to be crack initiation in the reaction layer causing stress concentrations on the fiber surface and fiber failure at relatively low stresses.

3. Continuous thermal exposure did not significantly alter the strength, modulus, or fracture mode of the Bsc/Al specimens.

4. Cyclic thermal exposure degraded the strength of both materials, but the strength of the Bsc/Al was degraded to a lesser extent than the B/Al specimens. The unexposed specimens fractured in the noncumulative mode, characteristic of strong interfaces. The fracture of the thermally cycled specimens showed transition toward the cumulative mode, characteristic of weak interfaces. The modulus remained constant. The failure mechanism for these specimens appeared to be weakening of the interfacial strength by a reversing stress field induced by the differences in thermal expansion. Cyclic exposure degraded the strength of the B/Al specimens more than continuous exposure.

Langley Research Center
National Aeronautics and Space Administration
Hampton, VA 23665
September 20, 1977

REFERENCES

1. Kerr, J. R.; Haskins, J. F.; and Stein, B. A.: Program Definition and Preliminary Results of a Long-Term Evaluation Program of Advanced Composites for Supersonic Cruise Aircraft Application. Environmental Effects on Advanced Composite Materials, ASTM Spec. Tech. Publ. 602, c.1976, pp. 3-22.

2. Metcalfe, Arthur, G.; and Klein, Mark J.: Effect of the Interface on Longitudinal Tensile Properties. Interfaces in Metal Matrix Composites, Arthur G. Metcalfe, ed., Academic Press, Inc., 1974, pp. 125-168.

3. Dardi, Louis E.; and Kreider, Kenneth G.: Thermal Cycling in Boron-Aluminum Composites. New Horizons in Materials and Processing, Volume II of National SAMPE Symposium and Exhibition, Soc. Advance. Mater. & Process Eng., Apr. 1973, pp. 125-139.

4. Shahinian, P.: Thermal Fatigue of Aluminum-Boron Composites. SAMPE Q., vol. 2, no. 1, Oct. 1970, pp. 28-35.

5. Wright, M. A.; and Intwala, B. D.: The Effect of Elevated Temperatures on the Mechanical Properties of B-Al Composites. J. Mater. Sci., vol. 8, no. 7, July 1973, pp. 957-963.

6. Wright, M. A.: The Effect of Thermal Cycling on the Mechanical Properties of Various Aluminum Alloys Reinforced With Unidirectional Boron Fibers. Metall. Trans., vol. 6A, no. 1, Jan. 1975, pp. 129-134.

7. Royster, Dick M.; Wiant, H. Ross; and Bales, Thomas T.: Joining and Fabrication of Metal-Matrix Composite Materials. NASA TM X-3282, 1975.

8. Kreider, Kenneth G.; and Prewo, K. M.: Boron-Reinforced Aluminum. Metallic Matrix Composites, Kenneth G. Kreider, ed., Academic Press, Inc., 1974, pp. 399-471.

9. Herring, Harvey W.: Fundamental Mechanisms of Tensile Fracture in Aluminum Sheet Unidirectionally Reinforced With Boron Filament. NASA TR R-383, 1972.

10. Klein, M. J.; Metcalfe, A. G.; and Gulden, M. E.: Effect of Interfaces in Metal Matrix Composites on Mechanical Properties. AFML-TR-72-226, U.S. Air Force, Nov. 1972. (Available from DDC as AD 759 204.)

TABLE I.- ROOM-TEMPERATURE ULTIMATE TENSILE STRENGTH AND STAGE II MODULUS FOR CONTINUOUSLY EXPOSED SPECIMENS

Continuous exposure conditions		B/Al		Bsc/Al	
Temperature, K	Time, hr	UTS, GPa	Stage II modulus, GPa	UTS, GPa	Stage II modulus, GPa
No exposure		1.37 1.46 1.36	244 247 245	1.11 1.33 1.41	251 238 239
728	80	1.23 1.31 1.25	232 235 234	1.11 1.24 1.09	239 239 251
	120	1.23 1.18 1.25	234 234 238	1.26 1.29 1.33	251 245 247
	160	1.17 1.19 1.08	239 233 226	1.26 1.06 1.29	246 246 251
	200	1.05 1.01 1.06	239 238 239	1.32 1.09 1.32	248 244 246
	240	0.98 1.01 .98	238 243 243	1.41 1.24 1.04	248 251 243
783	5	1.03 .90 1.09	263 257 243	1.39 1.26 1.41	250 253 243
	8	0.97 .85 .95	239 237 240	1.27 1.26 1.15	251 241 250
	10	0.76 .93 .83	245 257 239	1.10 1.48 1.41	242 251 246
	12	0.80 .87 .88	234 239 239	1.17 1.12 1.23	246 251 248

TABLE II.- ROOM-TEMPERATURE ULTIMATE TENSILE STRENGTH AND STAGE II MODULUS FOR CYCLICALLY EXPOSED SPECIMENS

Number of cycles between 293 K and 728 K	B/Al		Bsc/Al	
	UTS, GPa	Stage II modulus, GPa	UTS, GPa	Stage II modulus, GPa
0	1.65 1.56	174 185	1.22 1.37	191 191
1000	1.32 1.32	191 193	---- ----	--- ---
2057	1.21 1.19	192 185	1.12 ----	200 ---
6000	0.96 1.17	194 185	1.06 1.08	201 192

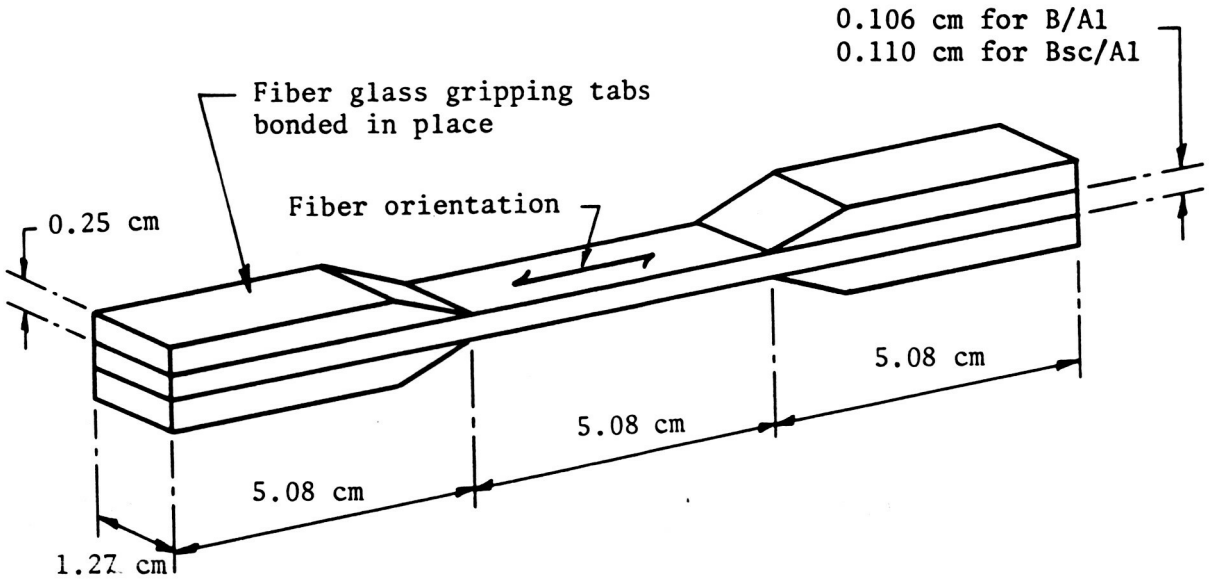

Figure 1.- Tensile test specimen.

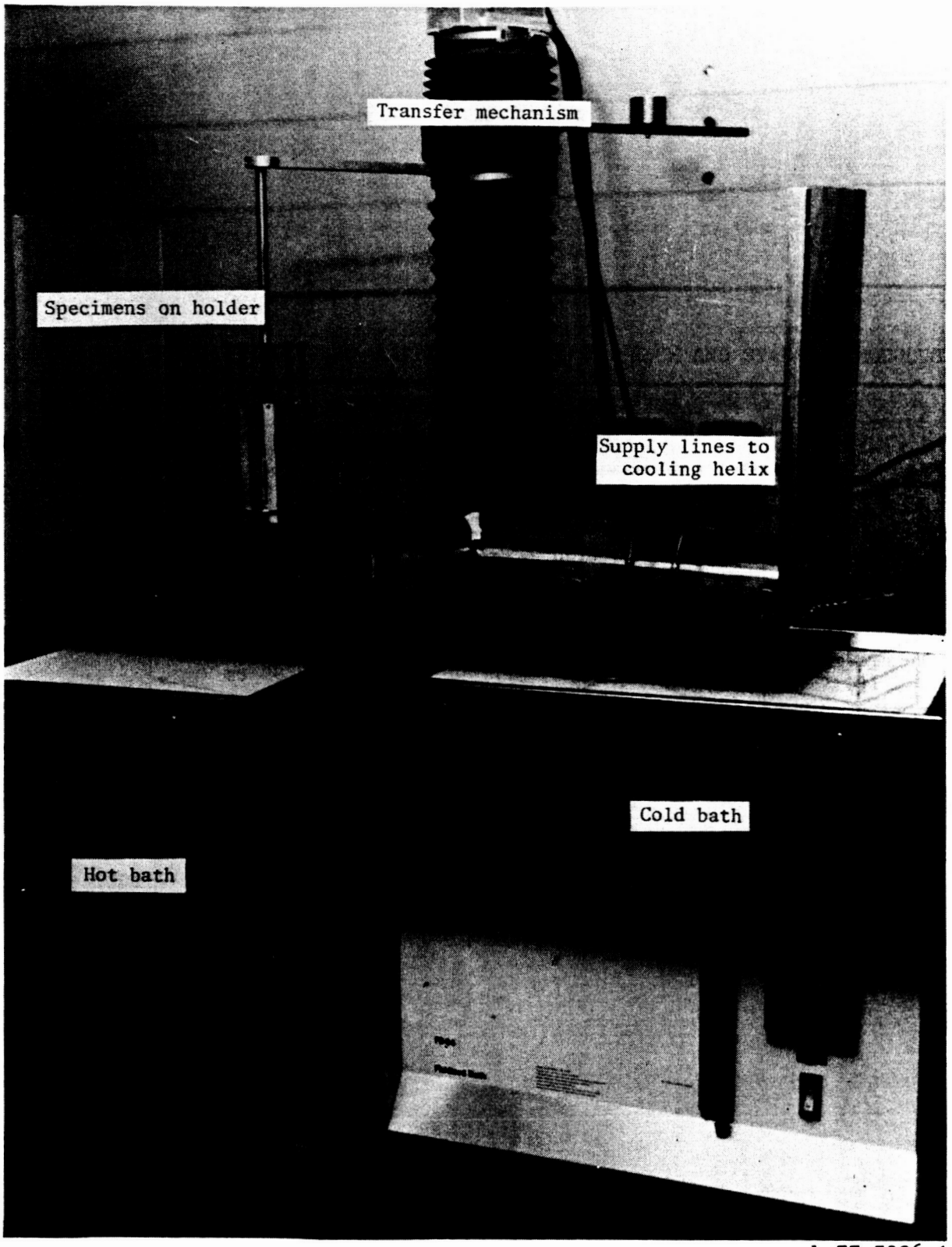

L-77-5036.1

Figure 2.- Thermal cycling apparatus.

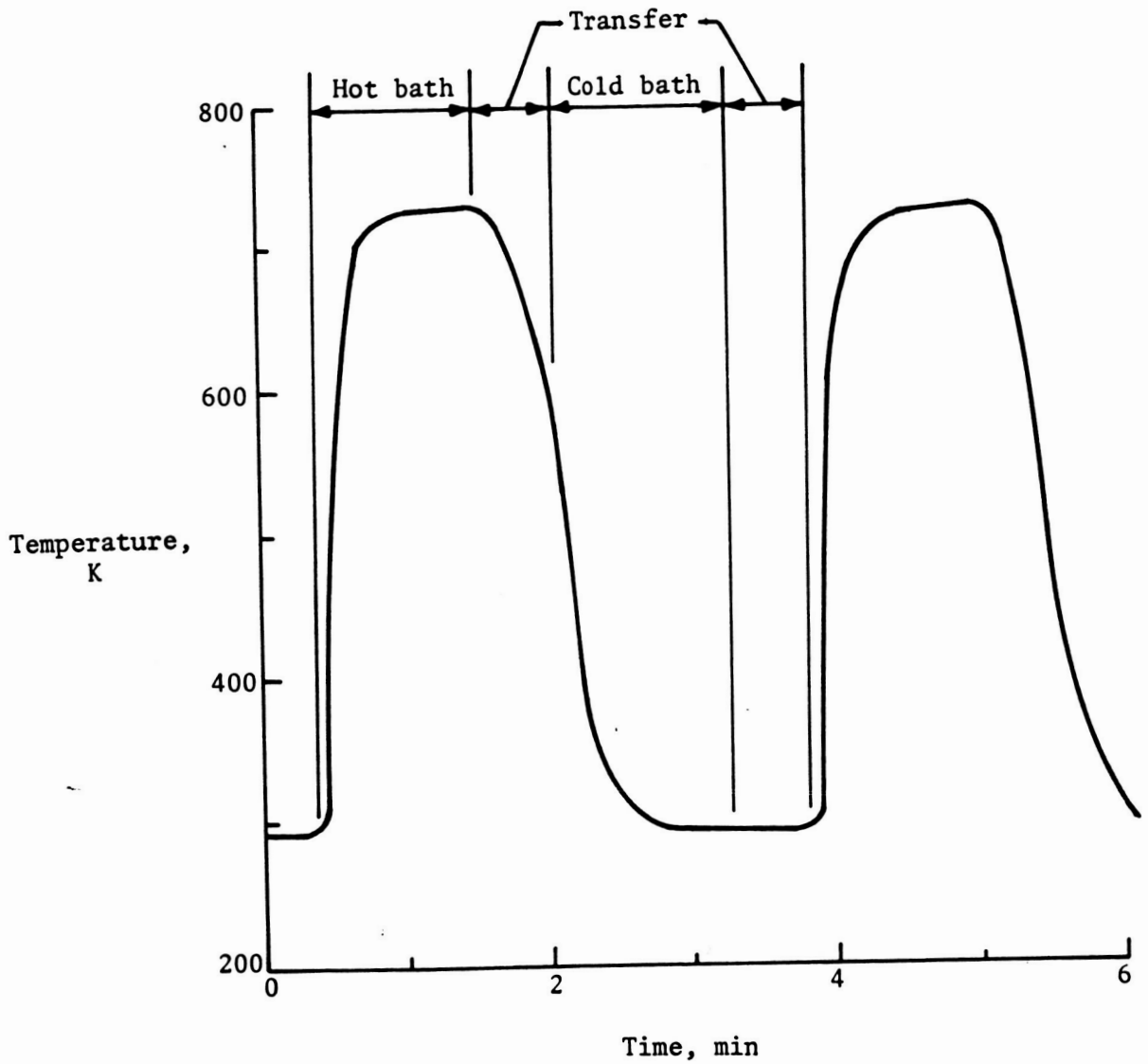

Figure 3.- Typical temperature history of specimen during thermal cycle in solid-particle fluidized bath.

Test Fixture Key

Mandrel no.	Corresponding strength range for 0.142-mm-diam boron fibers, GPa
0*	Less than 2.11
1	2.11 to 2.25
2	2.25 to 2.41
3	2.41 to 2.59
4	2.59 to 2.81
5	2.81 to 3.06
6	3.06 to 3.36
7	3.36 to 3.74
8	Greater than 3.74

* Fiber breaks on mandrel no. 1.

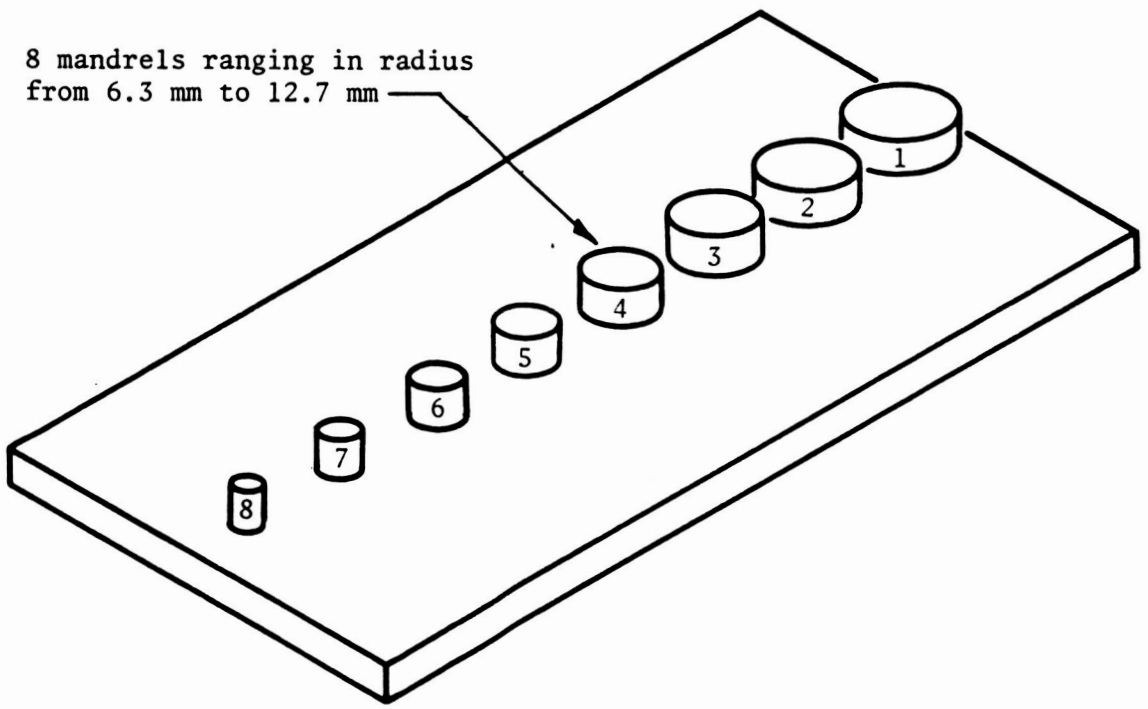

Figure 4.- Schematic of fiber strength test fixture.

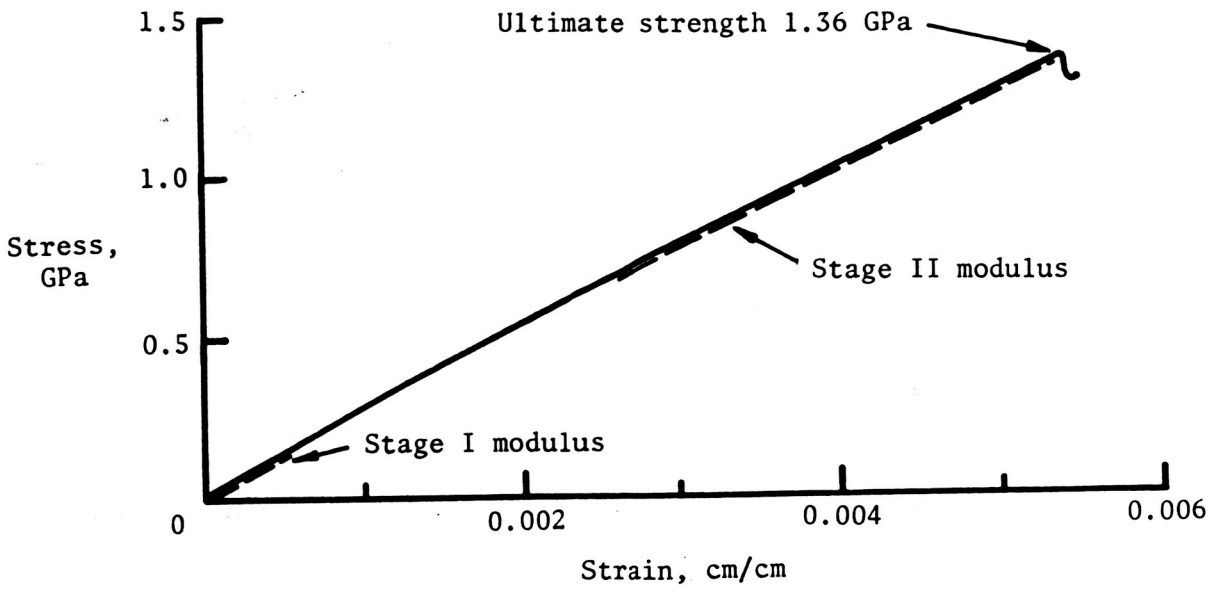

(a) No exposure.

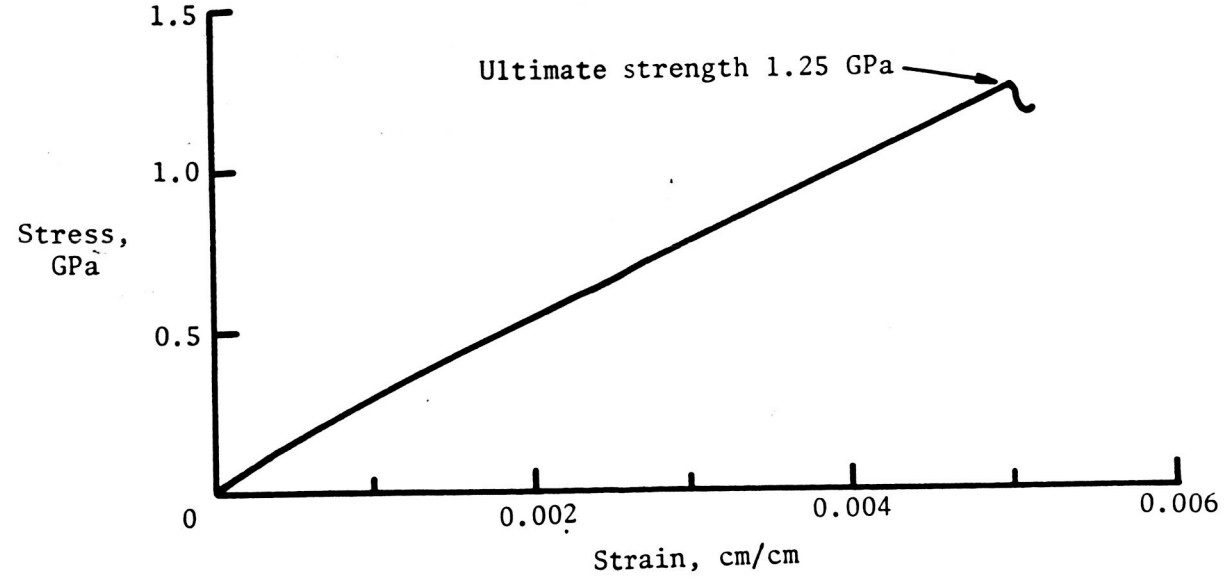

(b) Continuously exposed for 120 hr at 728 K.

Figure 5.- Typical tensile stress-strain curves for B/Al.

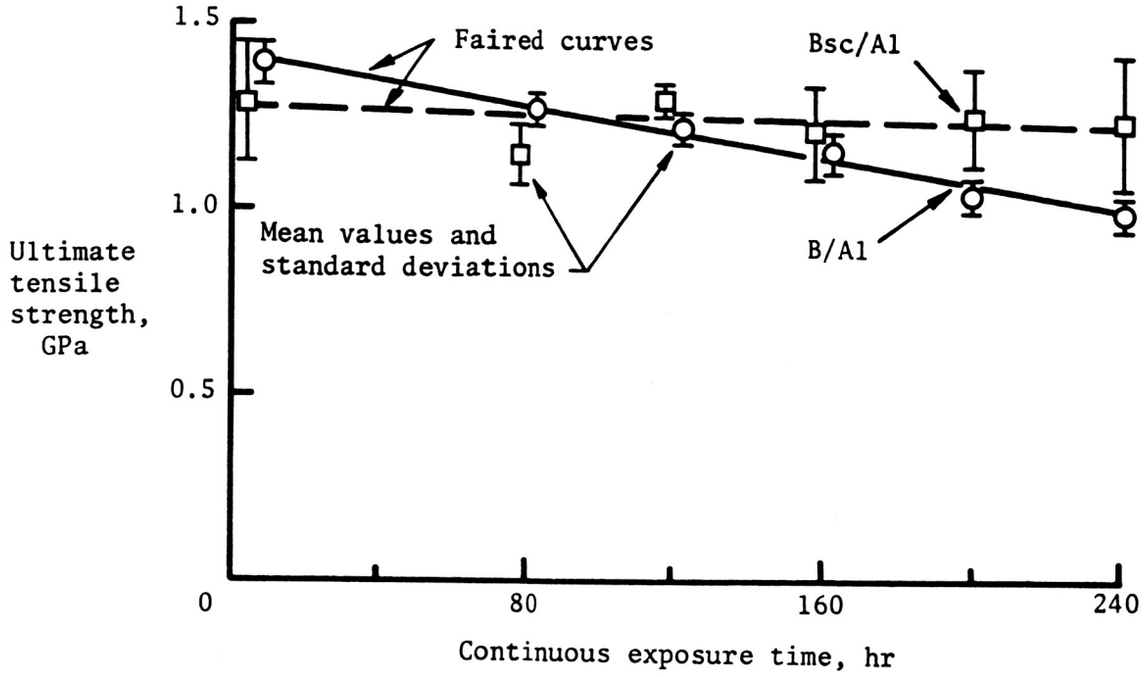

(a) 728 K.

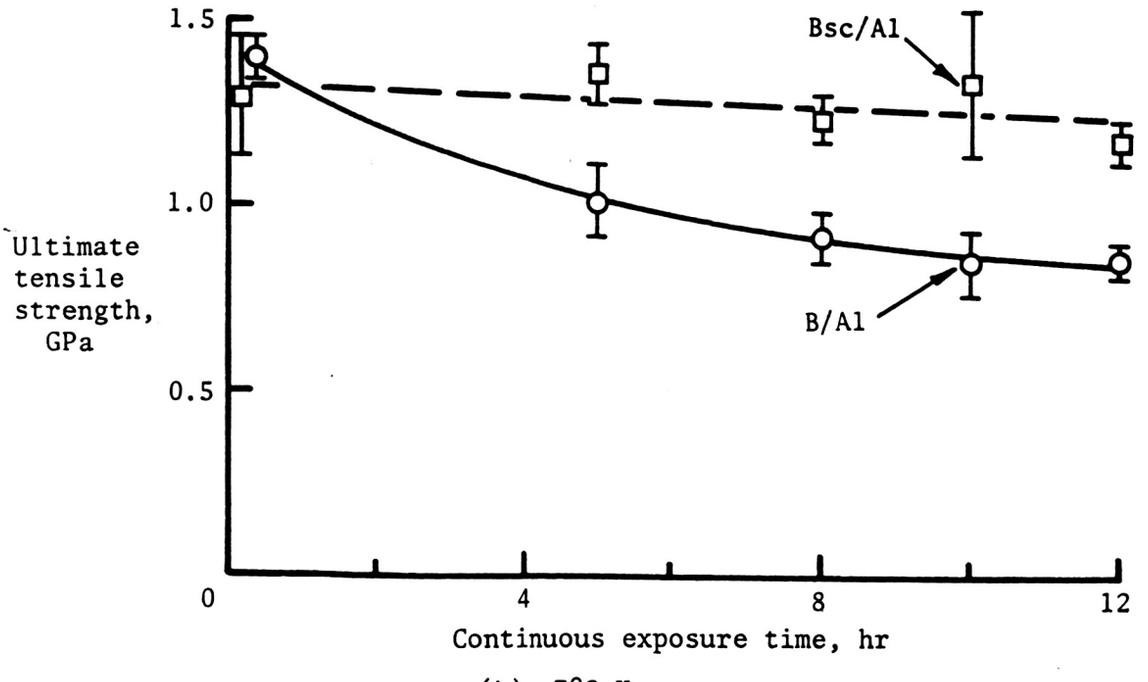

(b) 783 K.

Figure 6.- Ultimate tensile strength for continuously exposed B/Al and Bsc/Al.

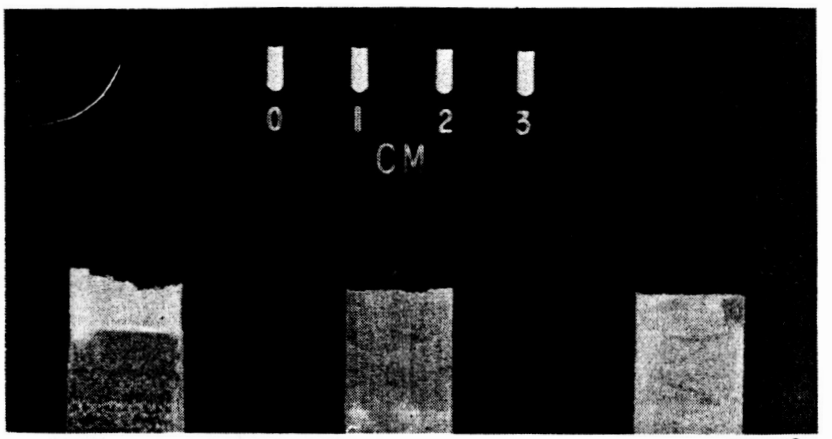

L-77-280

(a) No exposure. (b) 240 hr at 728 K. (c) 12 hr at 783 K.

Figure 7.- Fracture profiles of continuously exposed B/Al.

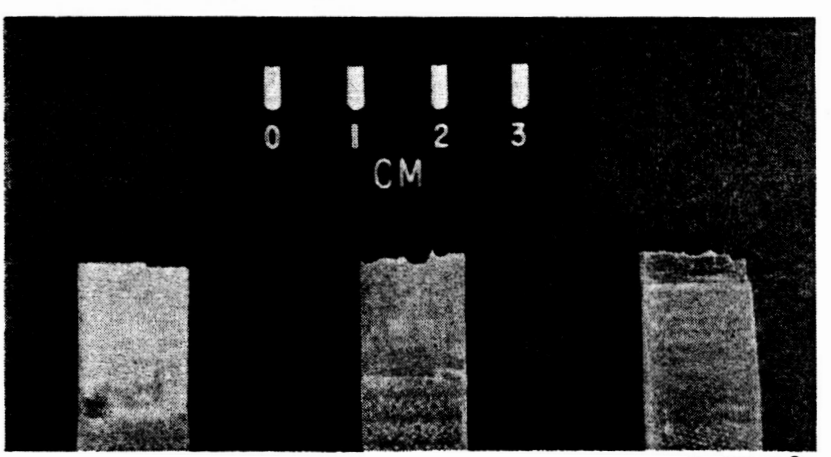

L-77-281

(a) No exposure. (b) 240 hr at 728 K. (c) 12 hr at 783 K.

Figure 8.- Fracture profiles of continuously exposed Bsc/Al.

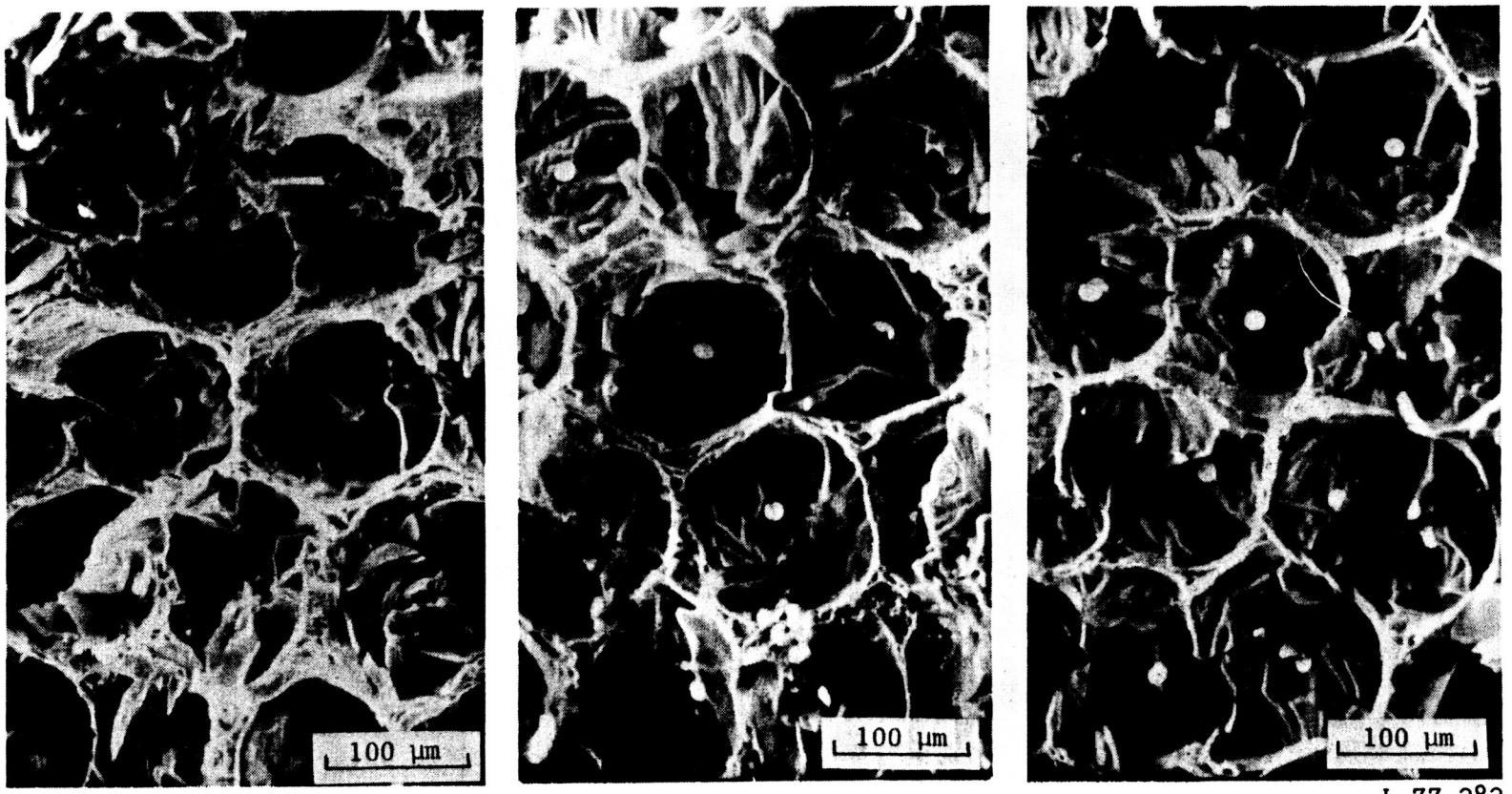

(a) No exposure. (b) 240 hr at 728 K. (c) 12 hr at 783 K.

Figure 9.- Fracture surfaces of continuously exposed B/Al.

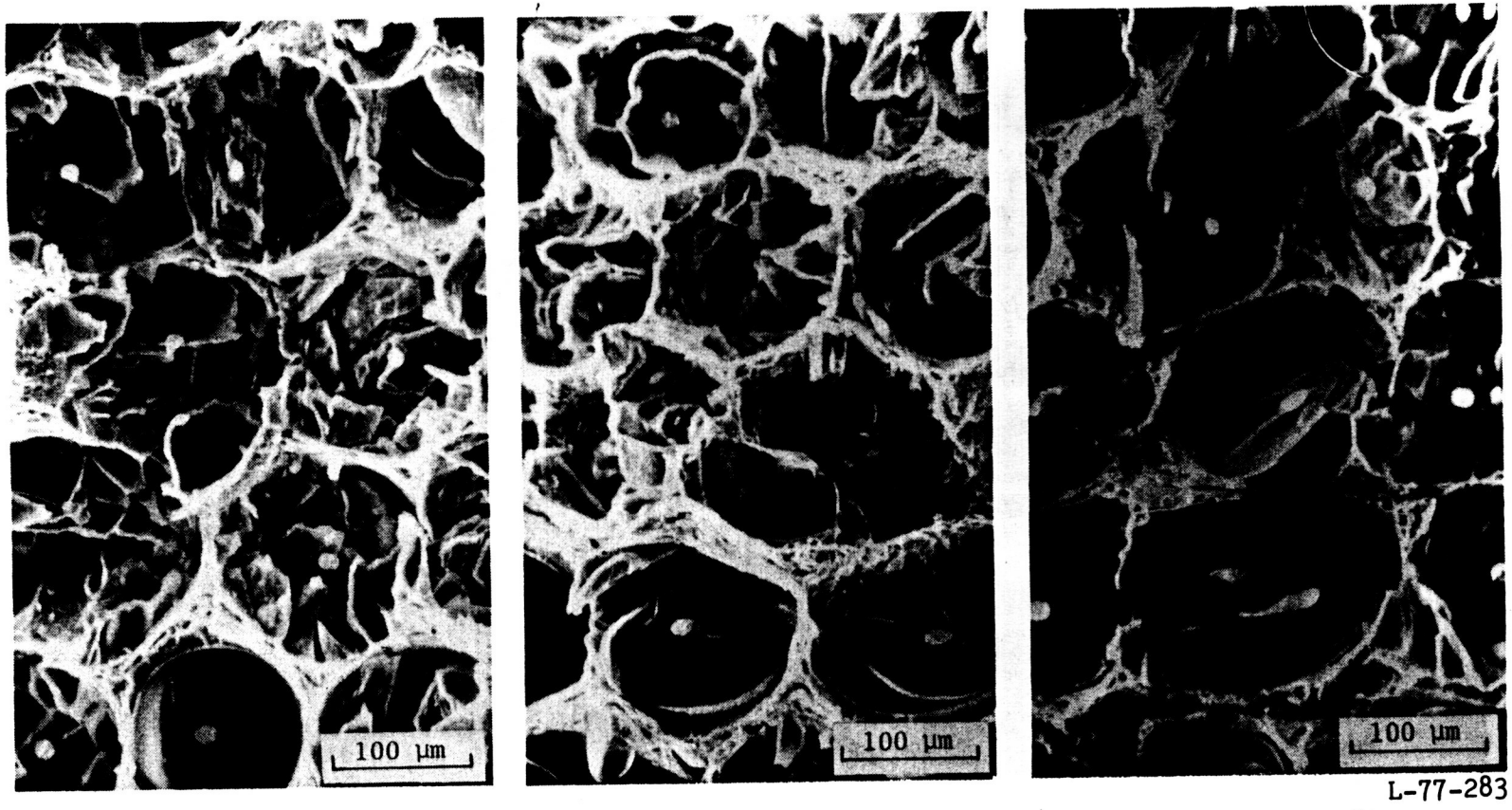

(a) No exposure. (b) 240 hr at 728 K. (c) 12 hr at 783 K.

Figure 10.- Fracture surfaces of continuously exposed Bsc/Al.

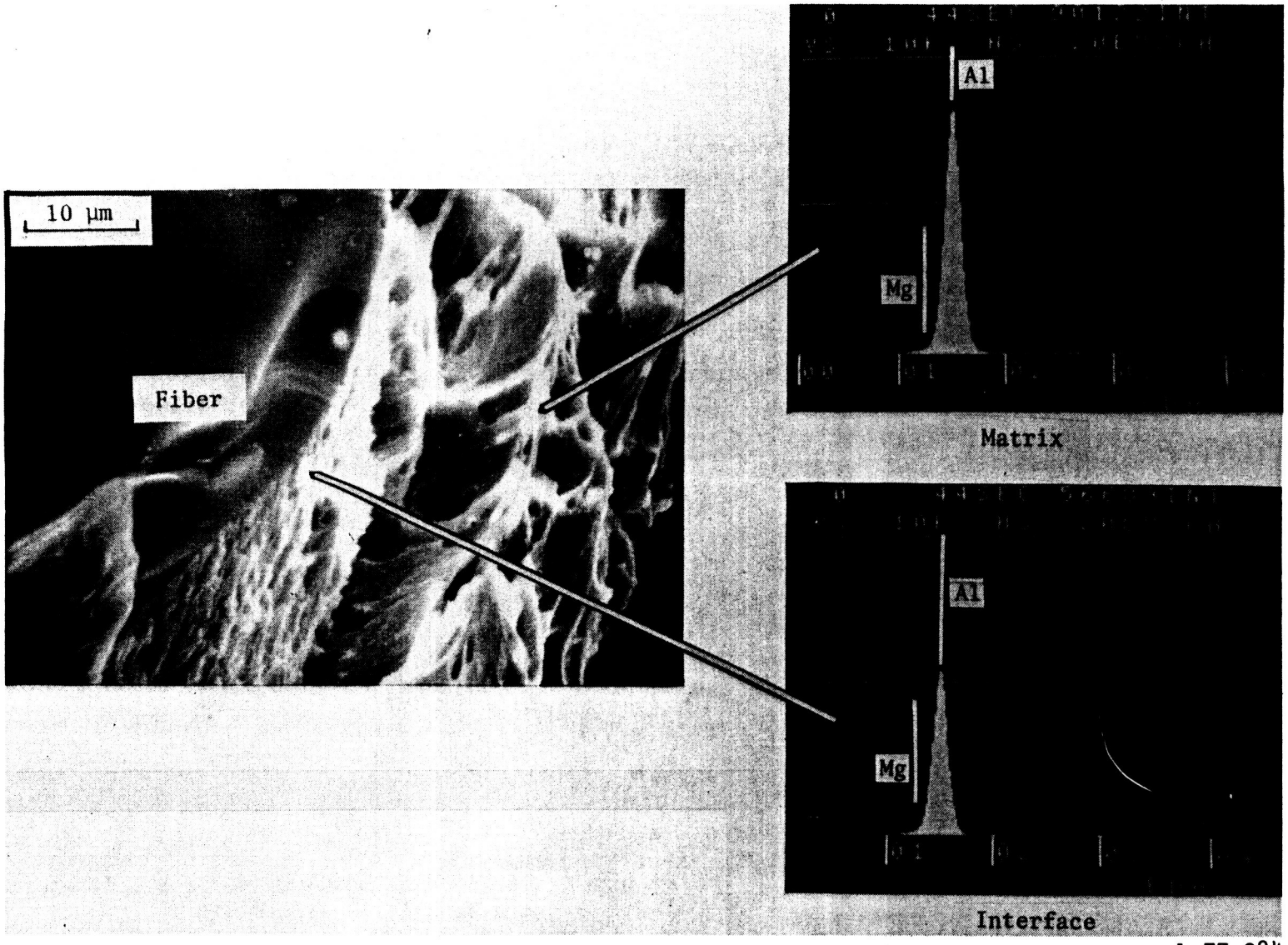

(a) No exposure.

Figure 11.- Fracture surface and EDAX spectra of B/Al continuously exposed at 728 K.

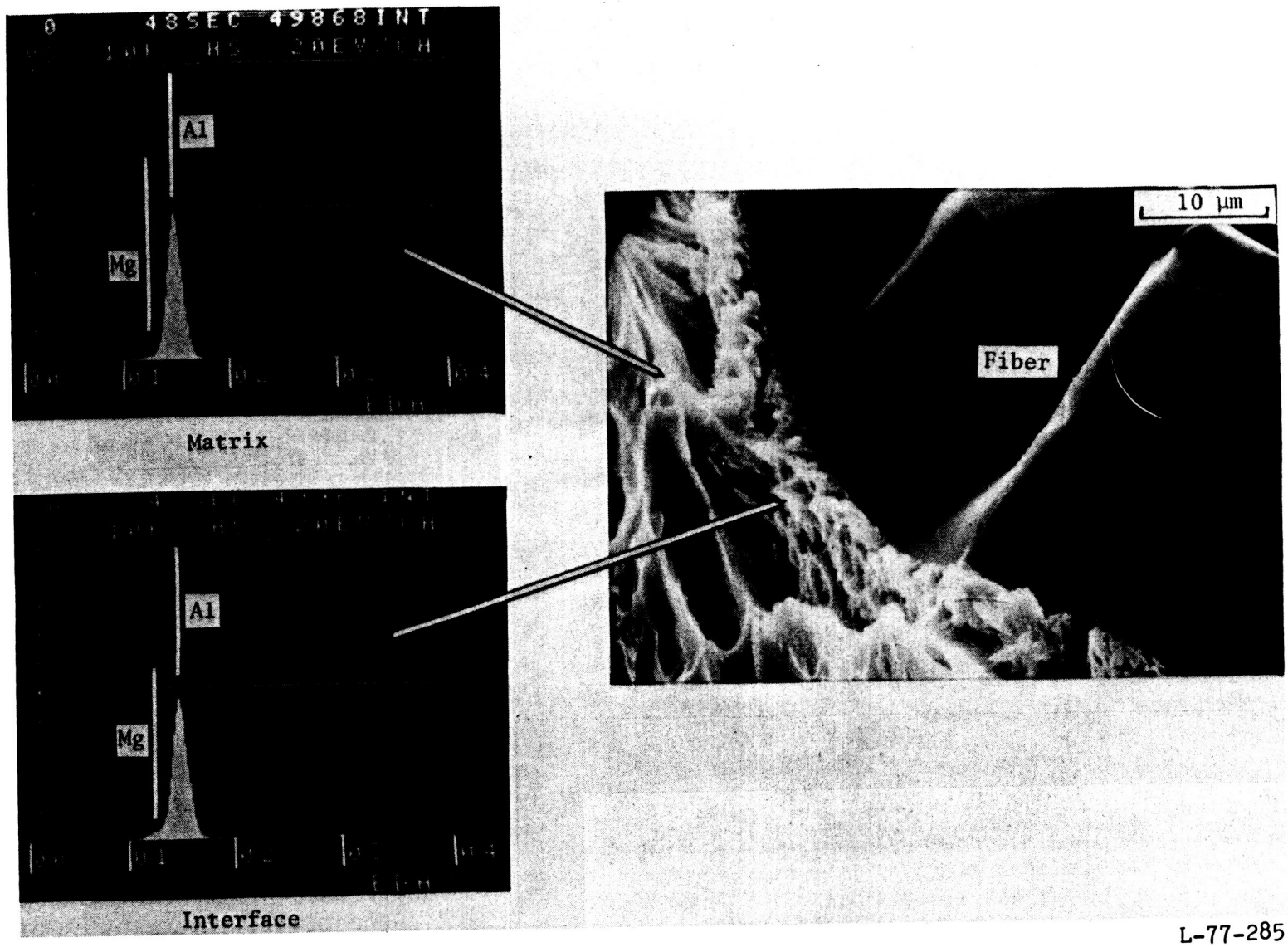

(b) 120 hr.

Figure 11.- Continued.

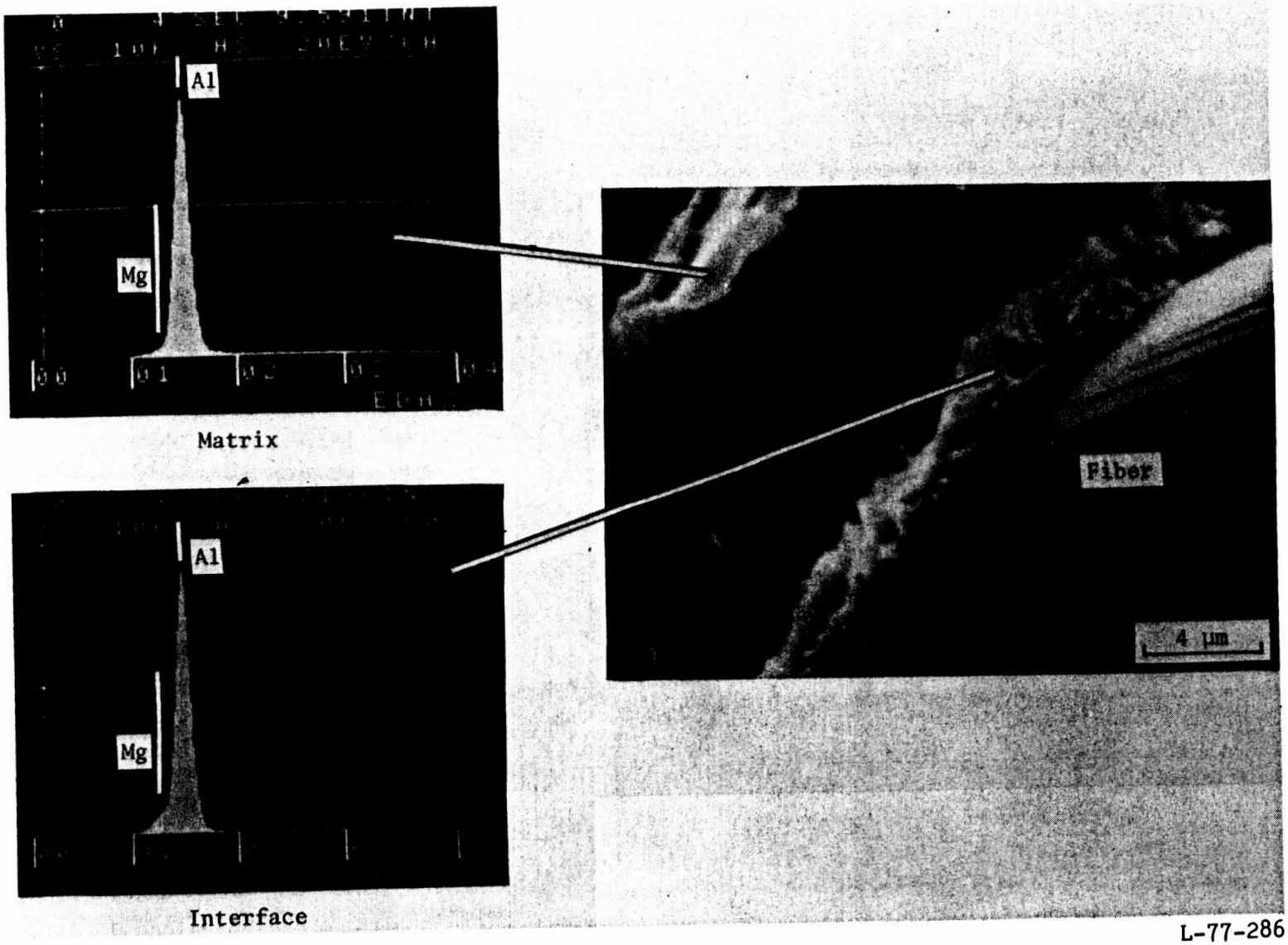

(c) 240 hr.

Figure 11.- Concluded.

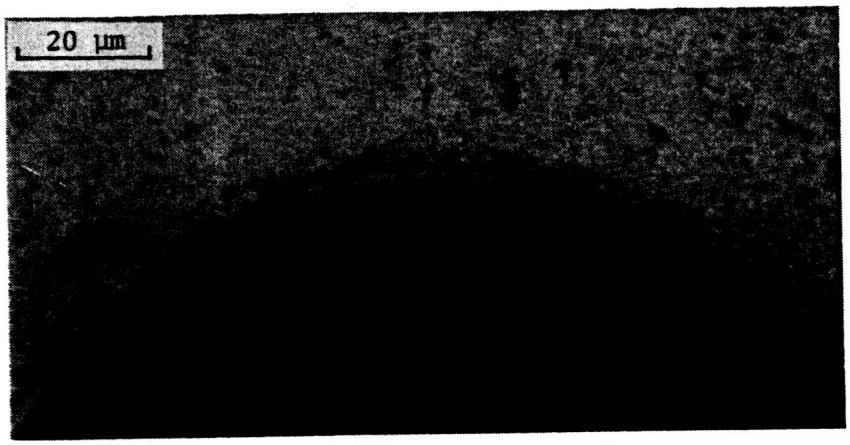

(a) No exposure.

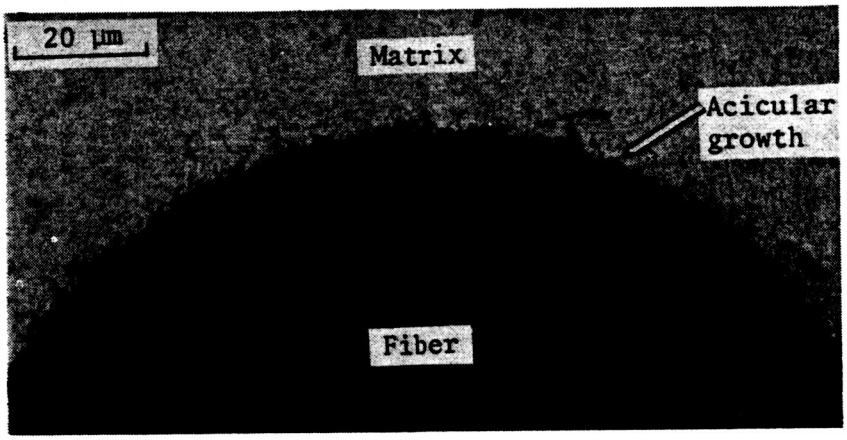

(b) 120 hr.

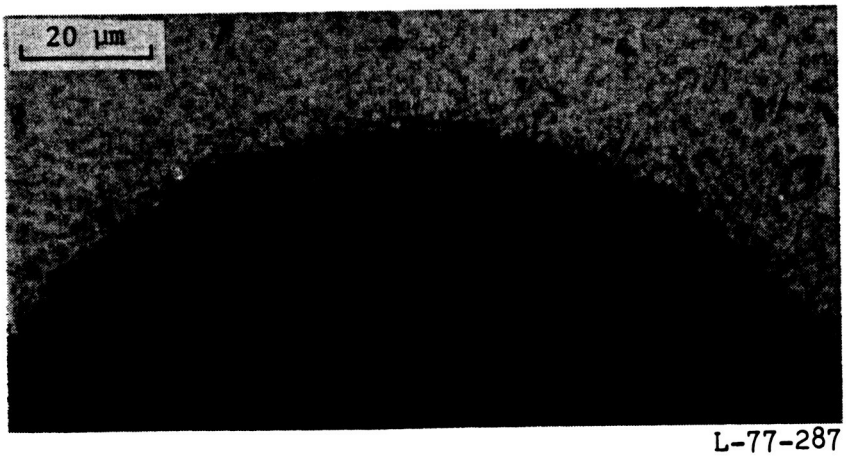

L-77-287

(c) 240 hr.

Figure 12.- Cross sections of B/Al continuously exposed at 728 K.

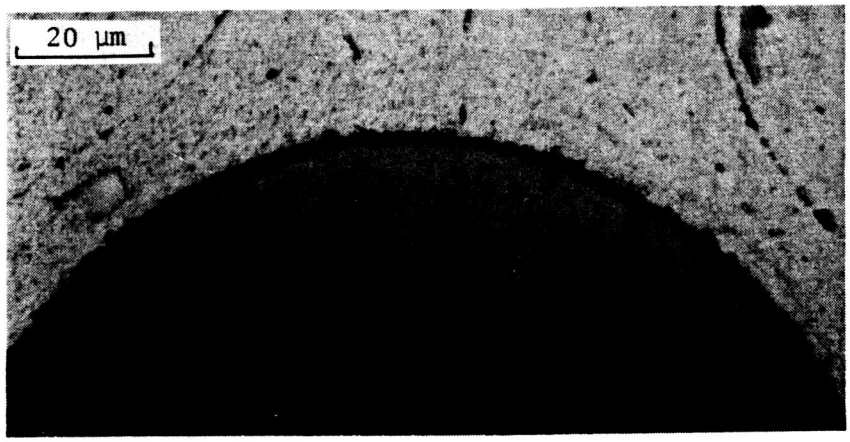

(a) No exposure.

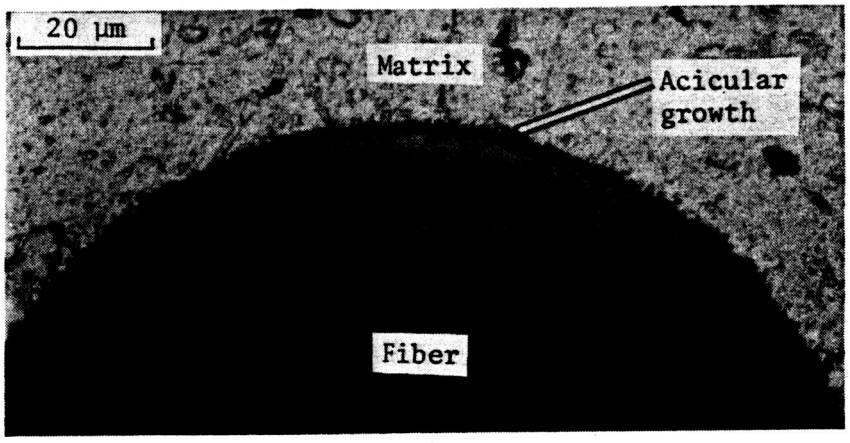

(b) 5 hr.

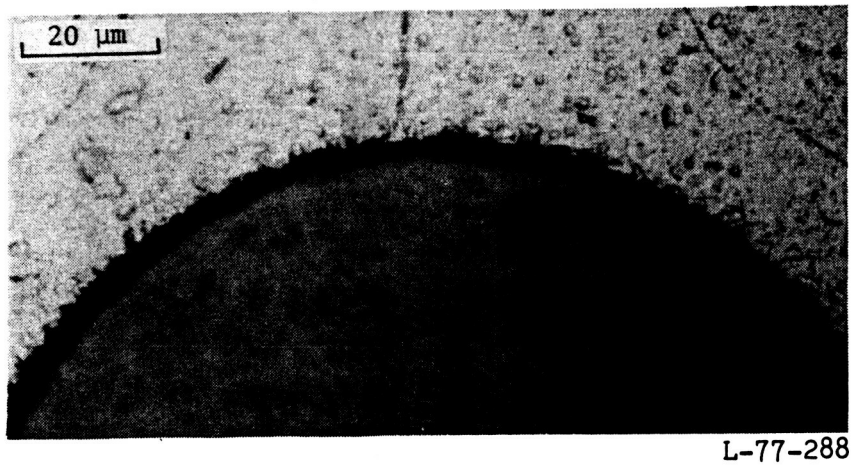

L-77-288

(c) 12 hr.

Figure 13.- Cross sections of B/Al continuously exposed at 783 K.

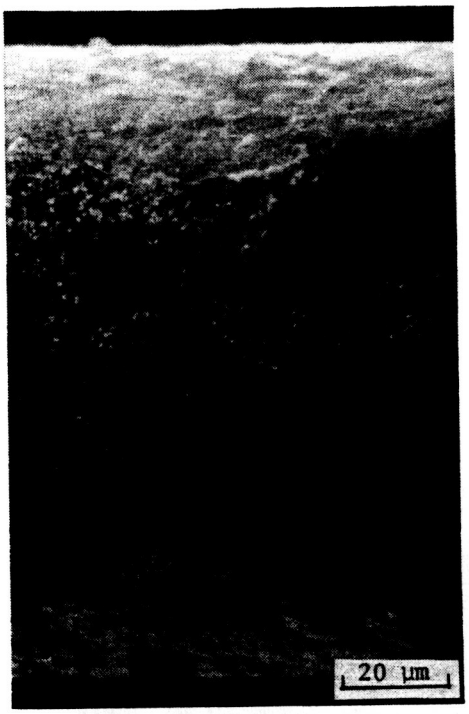

(a) No exposure.

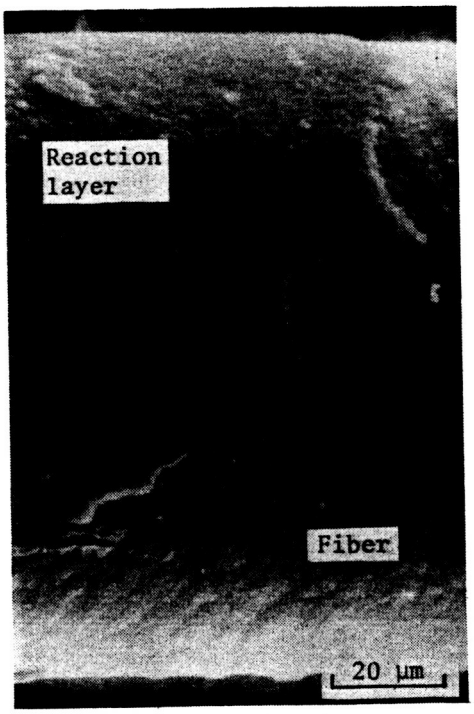

(b) 80 hr at 728 K.

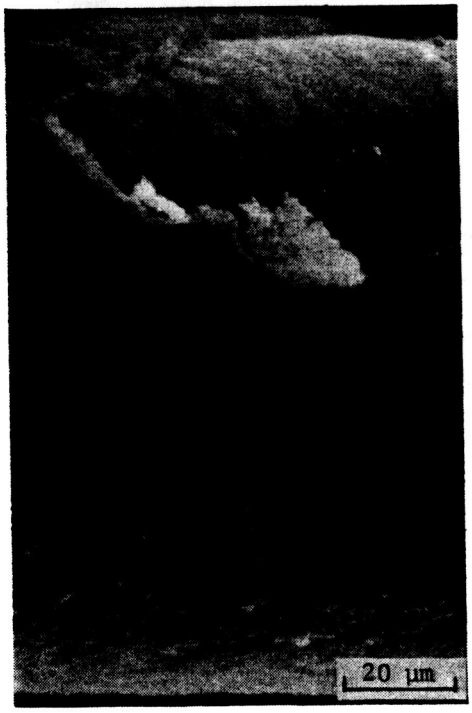

(c) 120 hr at 728 K.

L-77-289

(d) 240 hr at 728 K.

Figure 14.- Surface of fibers from continuously exposed B/Al.

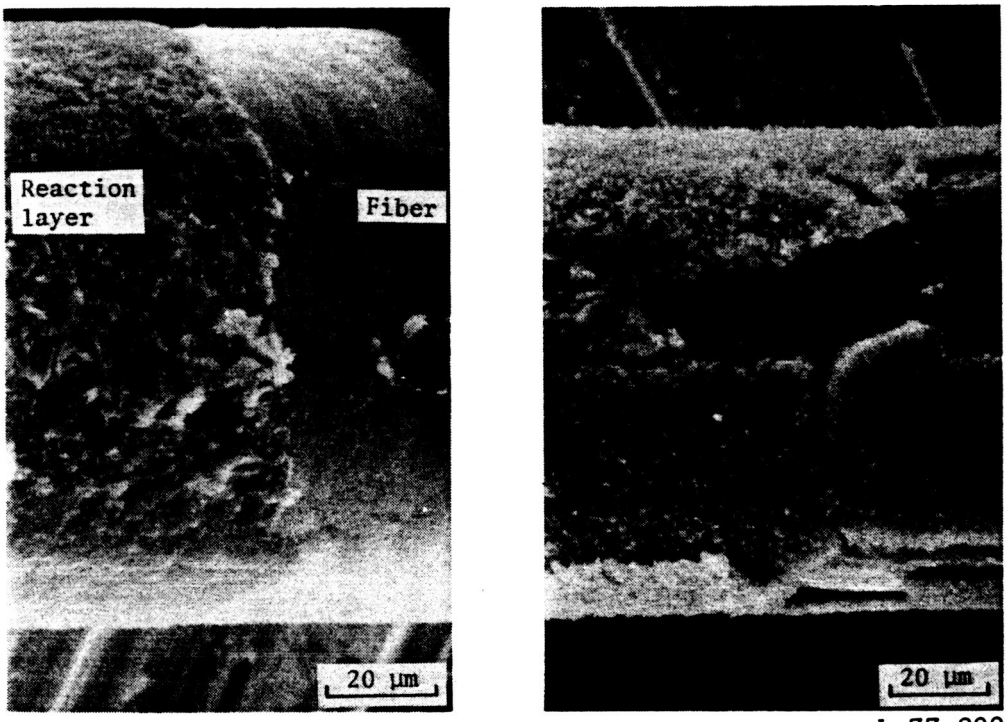

(e) 12 hr at 783 K.

(f) 170 hr at 783 K.

Figure 14.- Concluded.

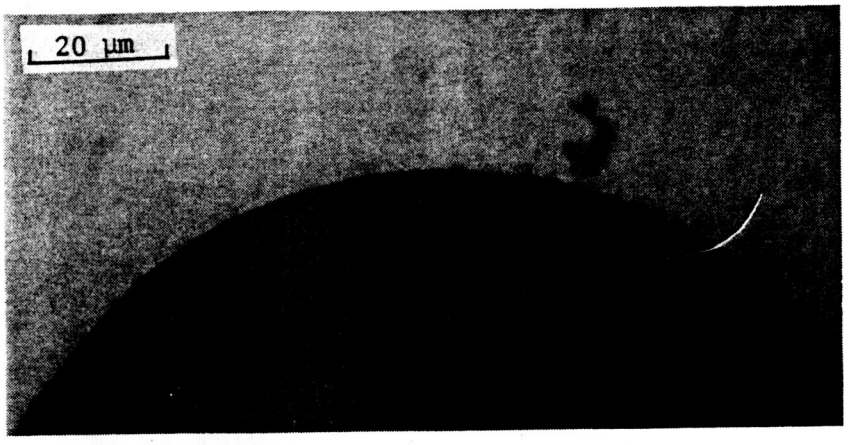

(a) No exposure.

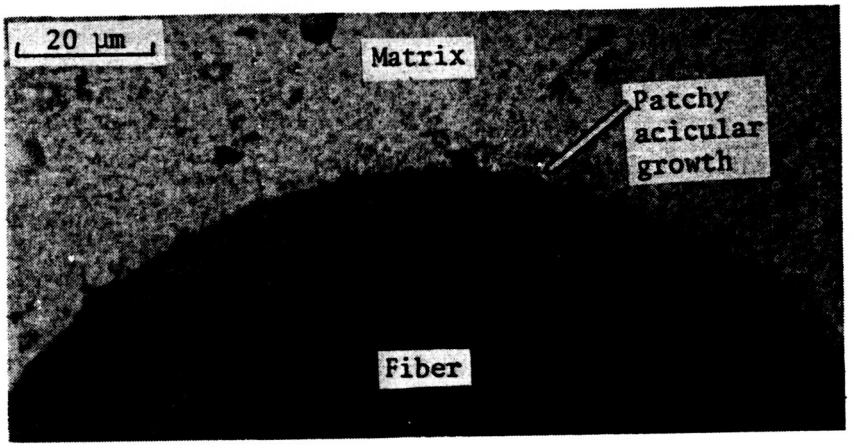

(b) 120 hr.

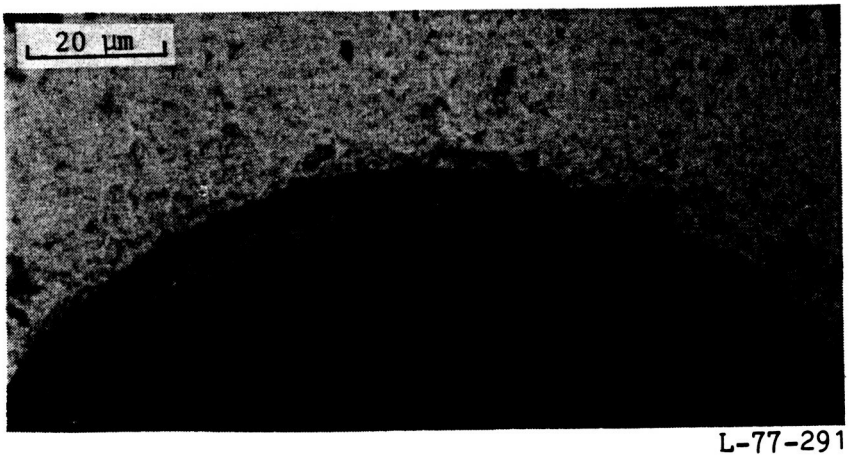

L-77-291

(c) 240 hr.

Figure 15.- Cross sections of Bsc/Al continuously exposed at 728 K.

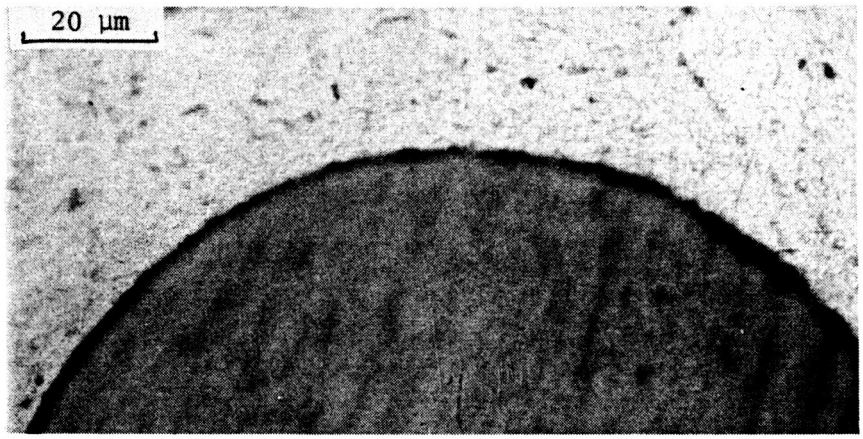

(a) No exposure.

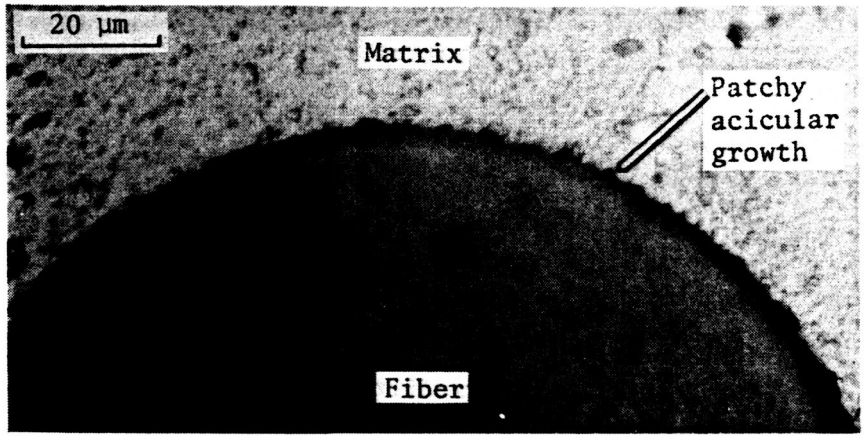

(b) 5 hr.

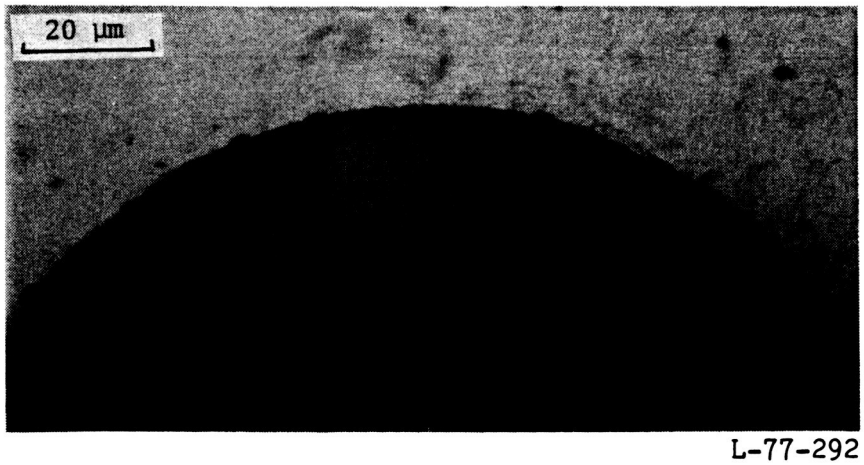

L-77-292

(c) 12 hr.

Figure 16.- Cross sections of Bsc/Al continuously exposed at 783 K.

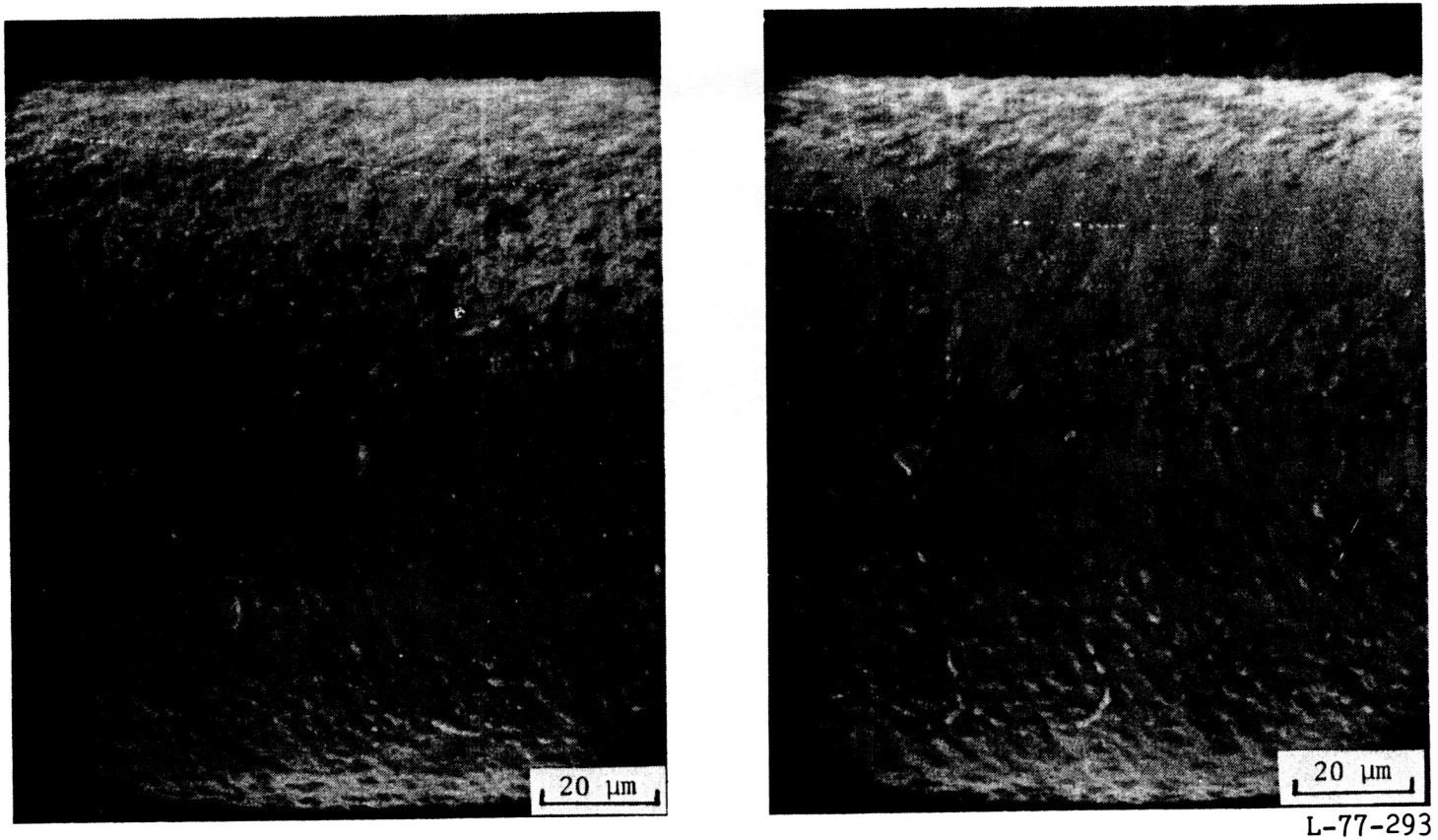

(a) No exposure, unetched.

(b) No exposure, etched.

Figure 17.- Surface of fibers from continuously exposed Bsc/Al.

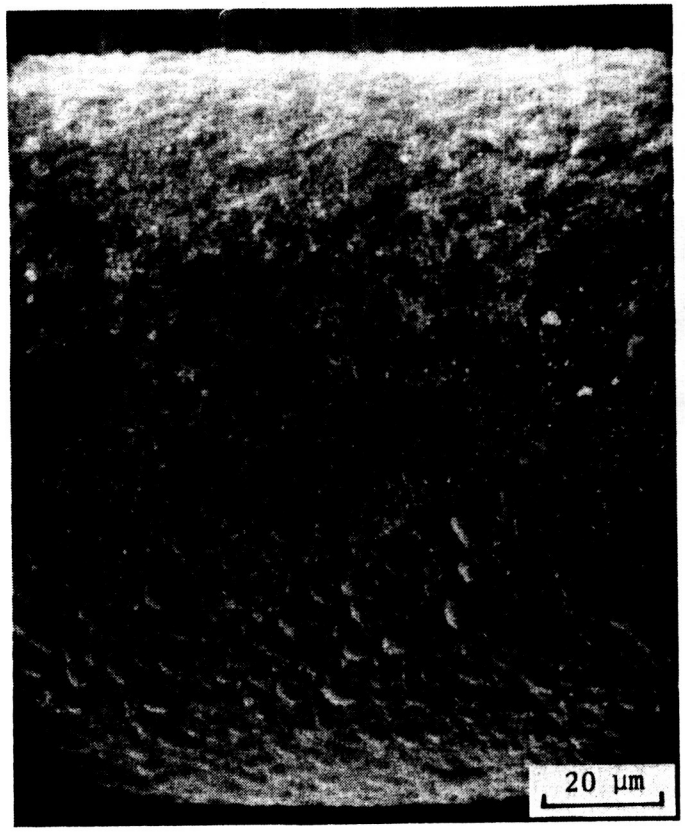

(c) 240 hr at 728 K, unetched.

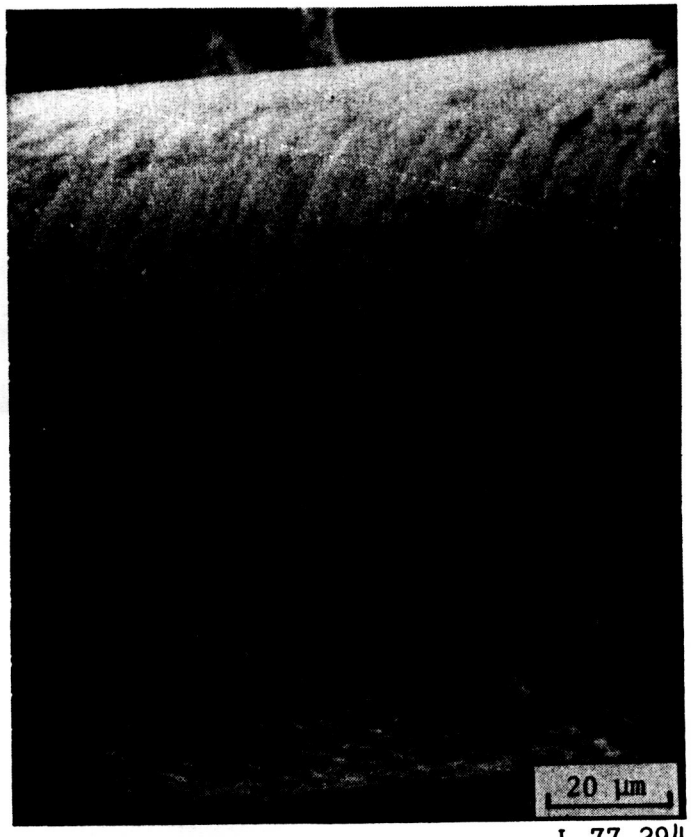

L-77-294

(d) 240 hr at 728 K, etched.

Figure 17.- Continued.

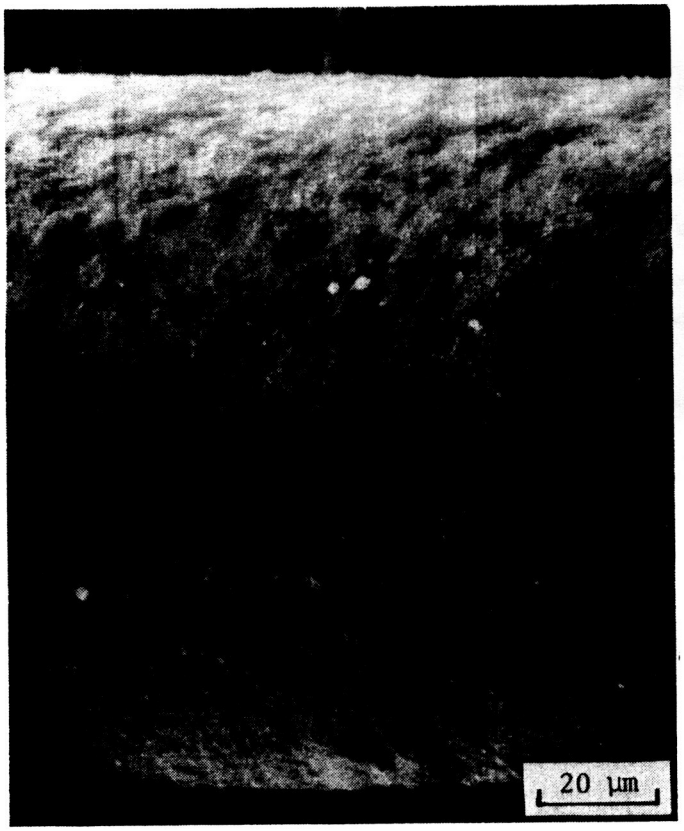

(e) 12 hr at 783 K, unetched.

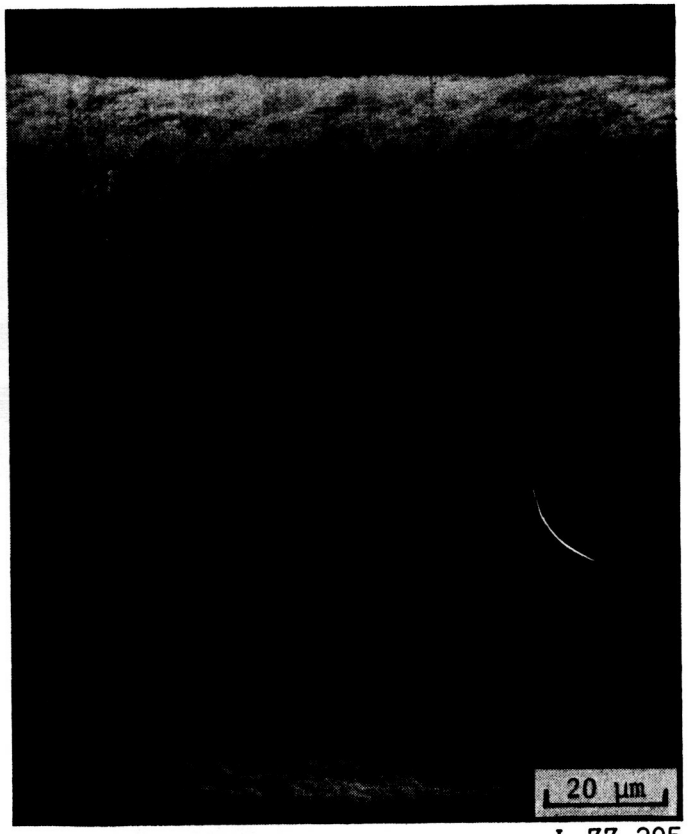

L-77-295

(f) 12 hr at 783 K, etched.

Figure 17.- Concluded.

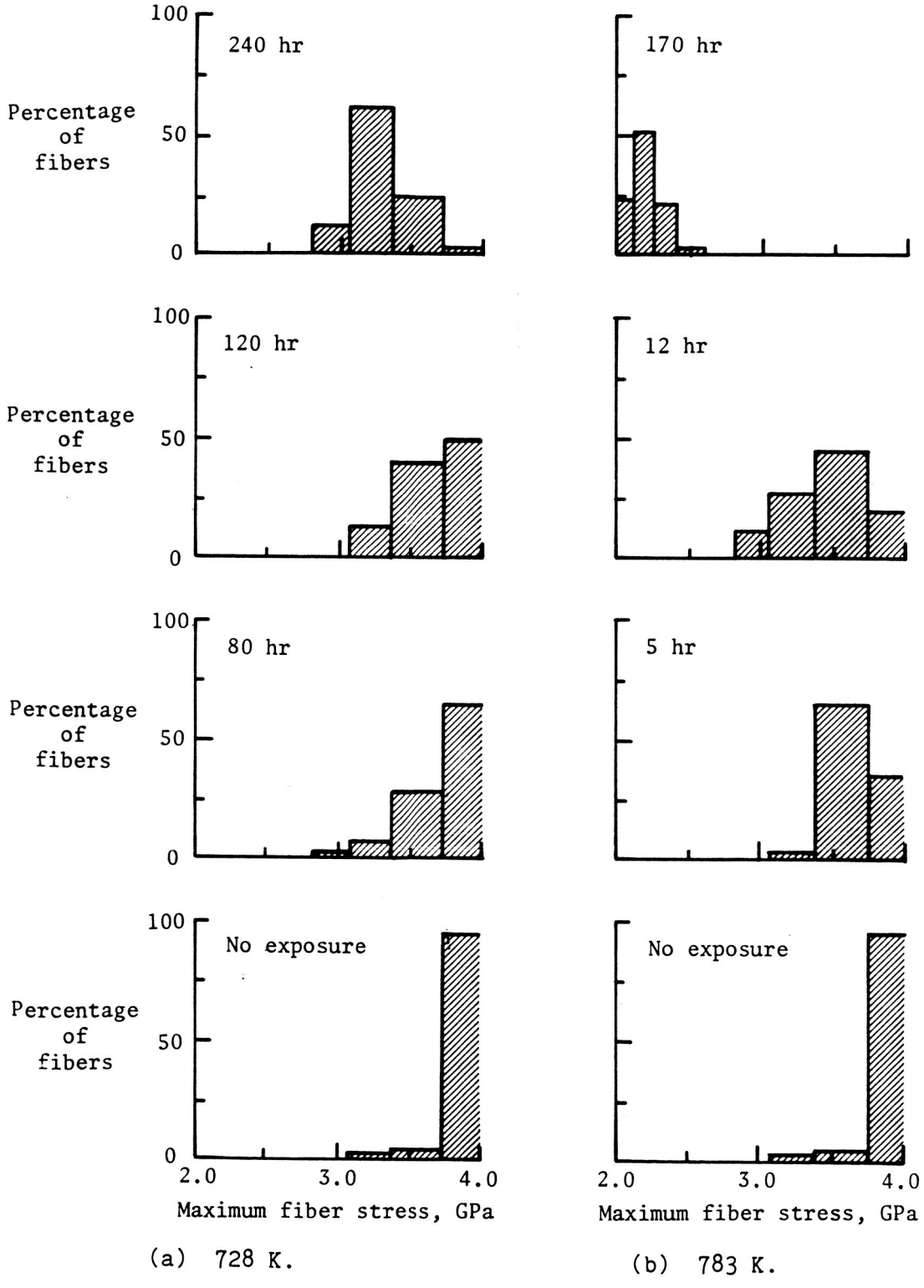

Figure 18.- Fiber strength distributions from continuously exposed B/Al.

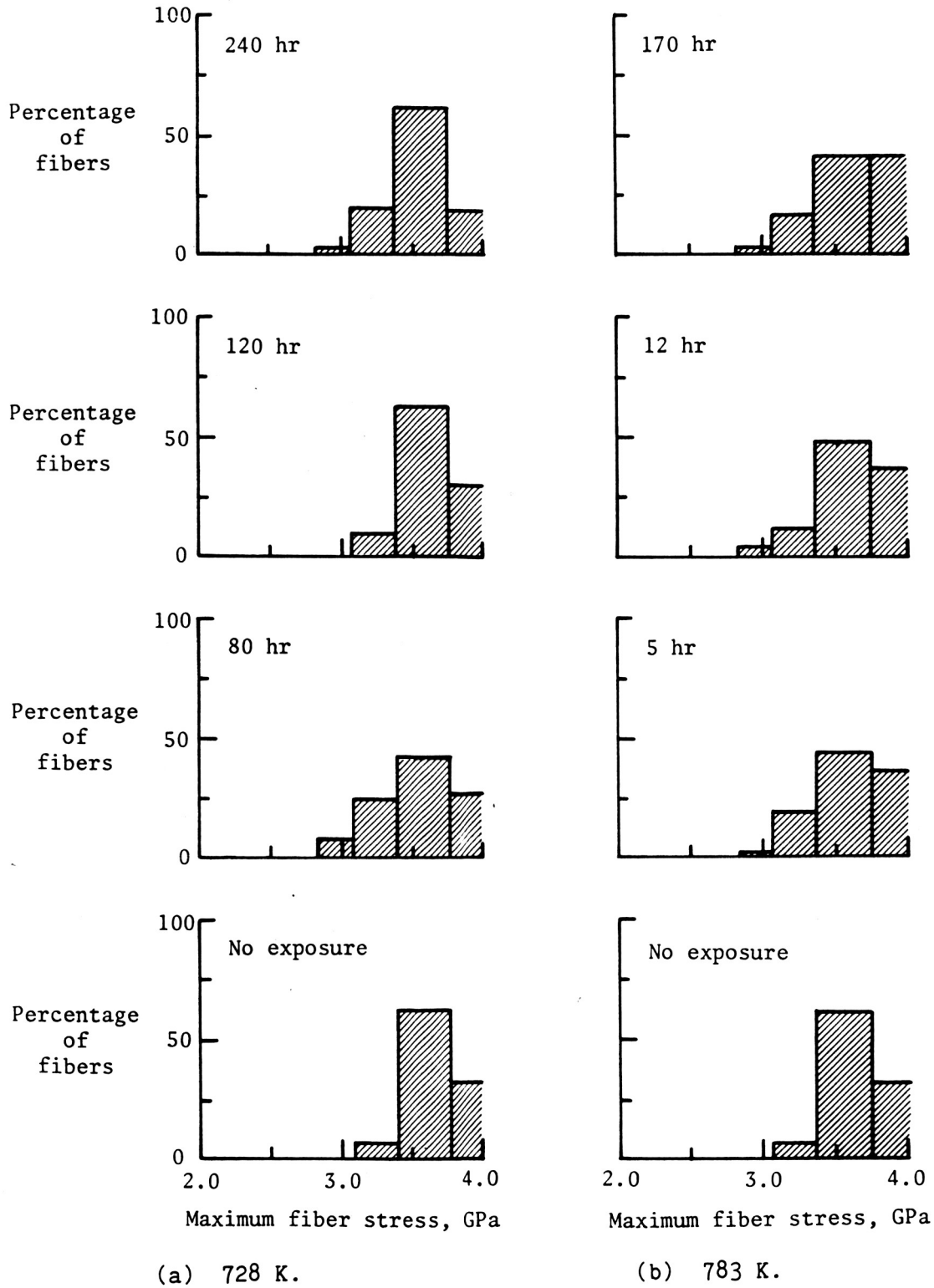

(a) 728 K. (b) 783 K.

Figure 19.- Fiber strength distributions from continuously exposed Bsc/Al.

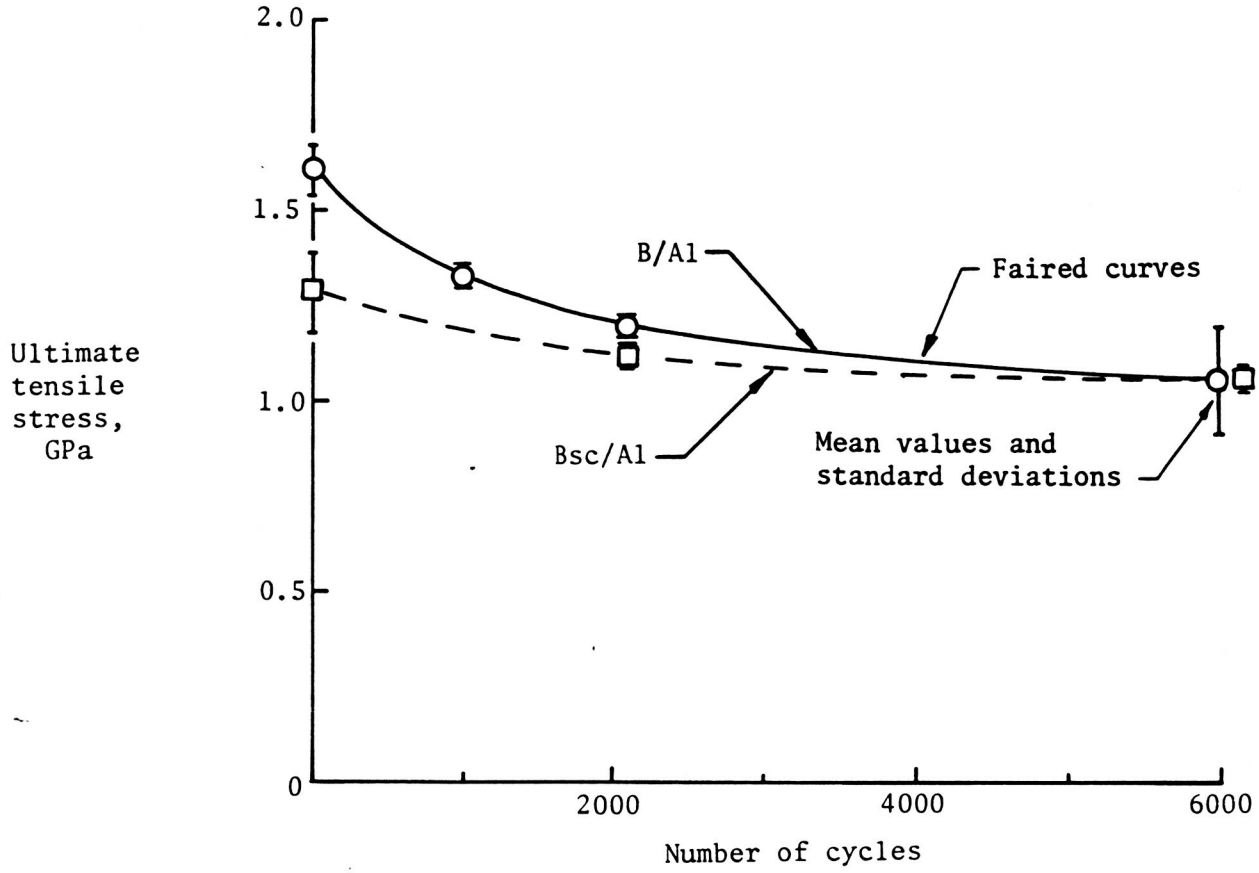

Figure 20.- Ultimate tensile strength for B/Al and Bsc/Al cyclically exposed between 293 K and 728 K.

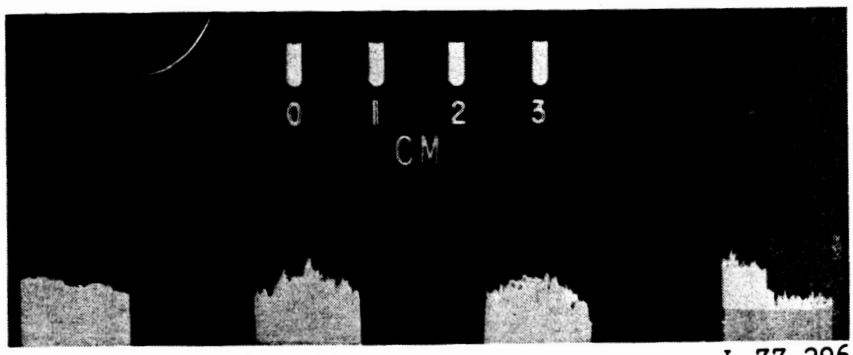

L-77-296

(a) No exposure. (b) 1000 cycles. (c) 2057 cycles. (d) 6000 cycles.

Figure 21.- Fracture profiles of B/Al cyclically exposed between 293 K and 728 K.

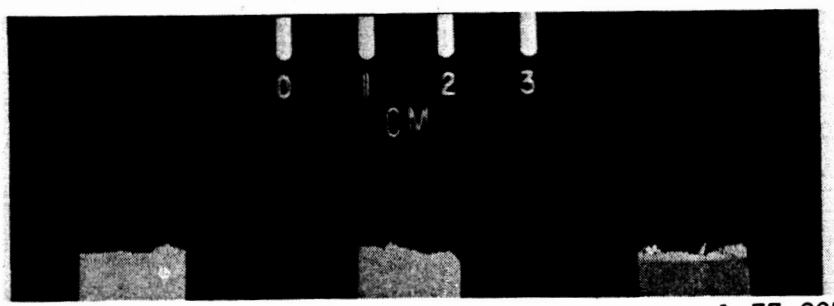

L-77-297

(a) No exposure. (b) 2057 cycles. (c) 6000 cycles.

Figure 22.- Fracture profiles of Bsc/Al cyclically exposed between 293 K and 728 K.

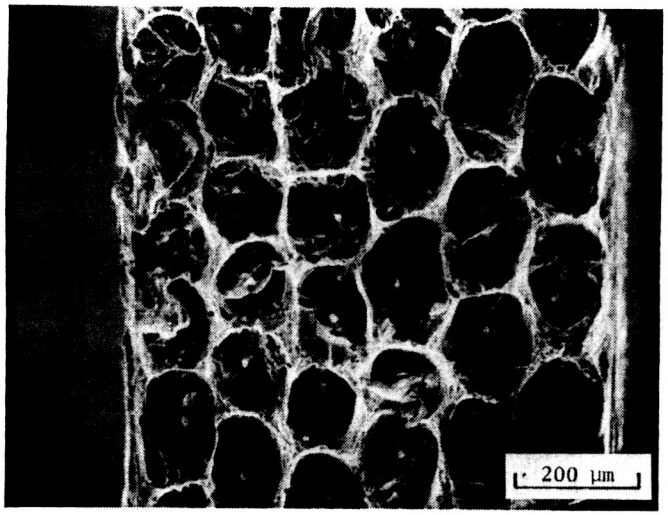

(a) No exposure.

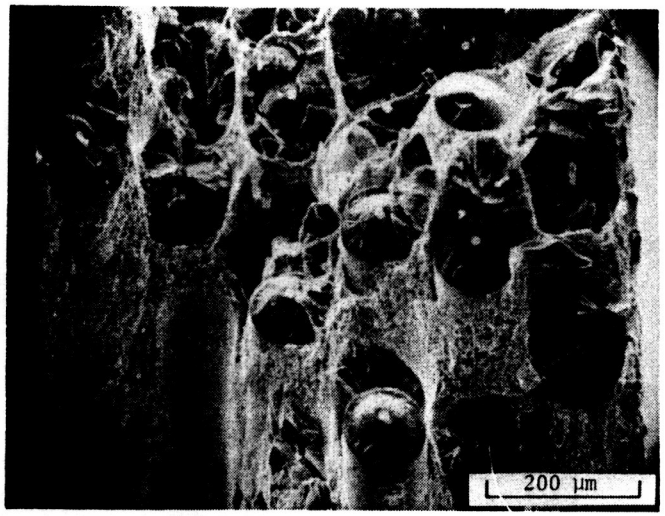

(b) 1000 cycles.

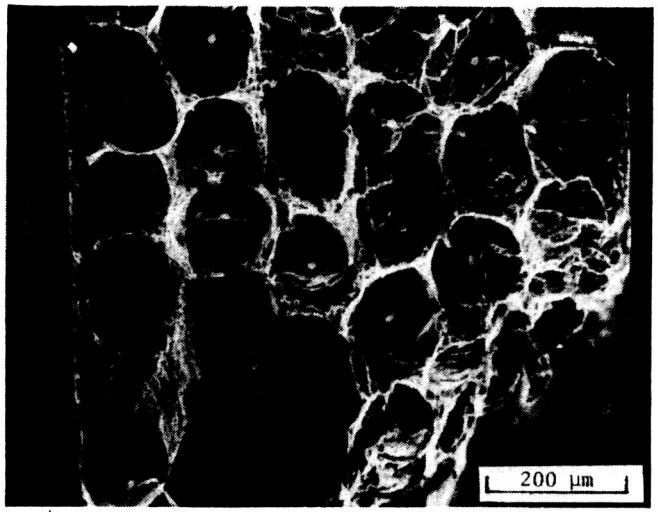

(c) 2057 cycles.

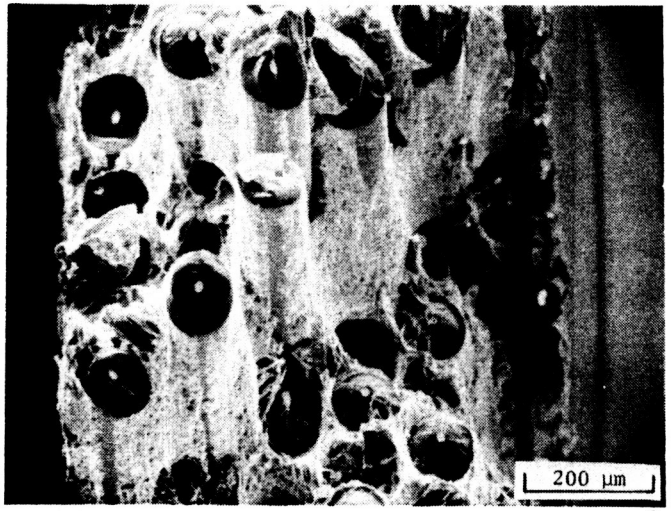

L-77-298

(d) 6000 cycles.

Figure 23.- Fracture surfaces of B/Al cyclically exposed between 293 K and 728 K.

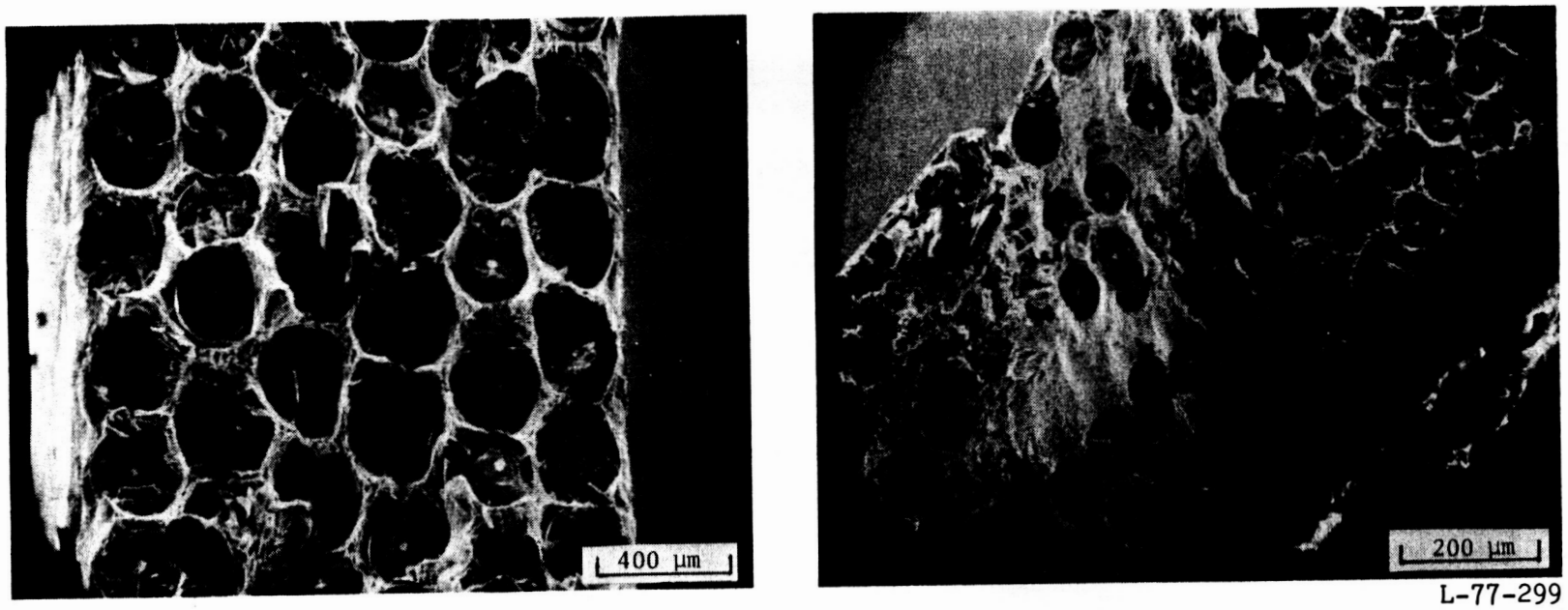

(a) No exposure.

(b) 6000 cycles.

Figure 24.- Fracture surfaces of Bsc/Al cyclically exposed between 293 K and 728 K.

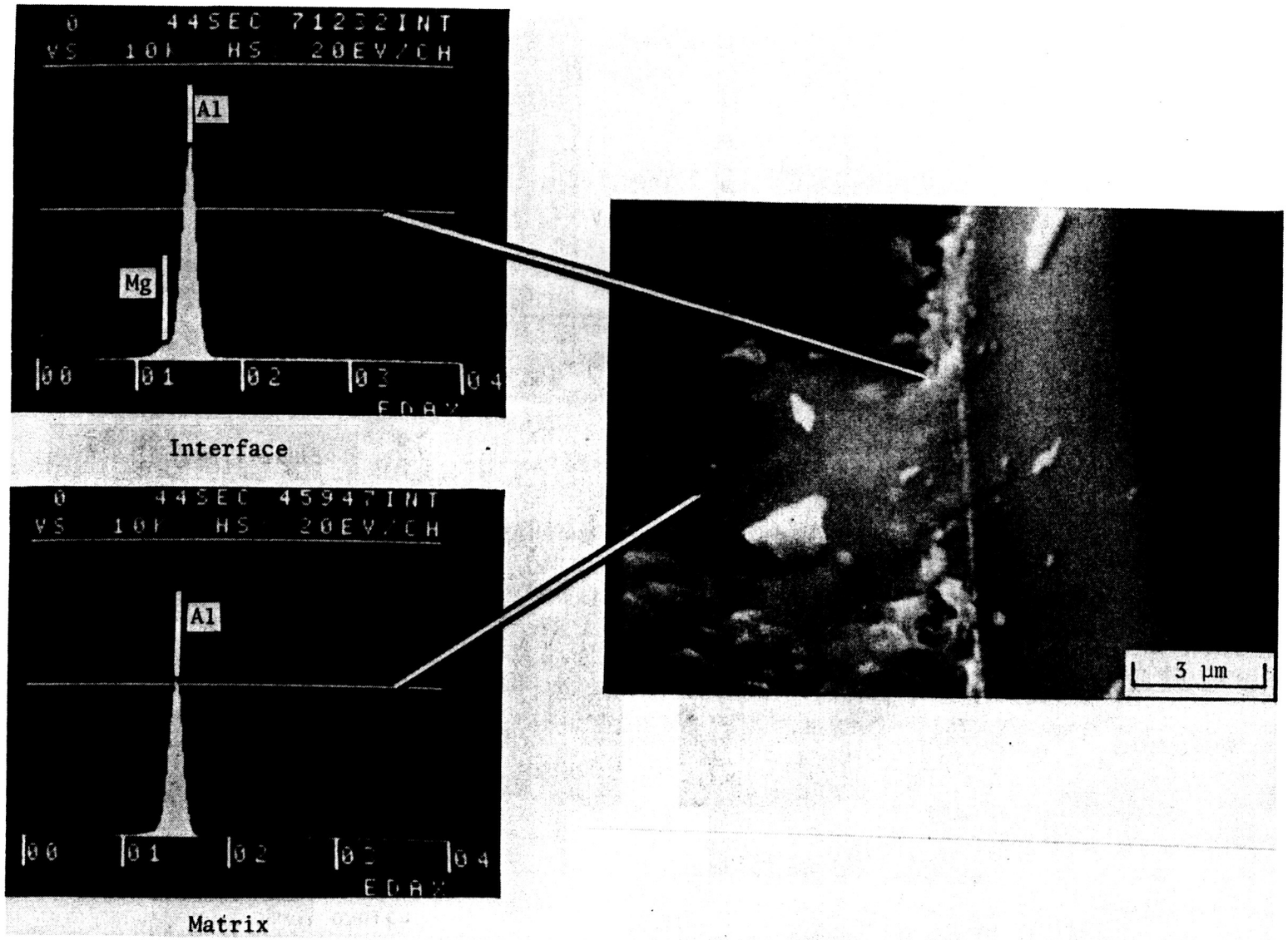

L-77-300

Figure 25.- Fracture surface and EDAX spectra of B/Al after 6000 cycles between 293 K and 728 K.

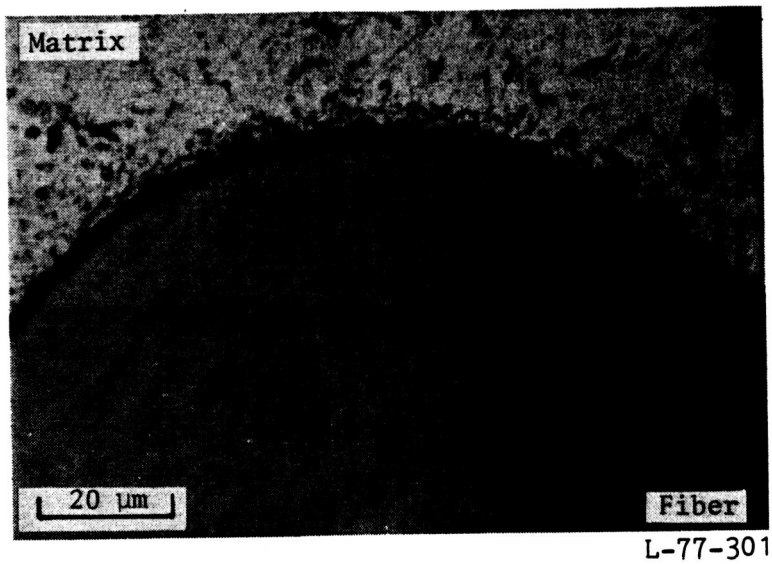

L-77-301

Figure 26.- Cross section of polished B/Al after 6000 cycles between 293 K and 728 K.

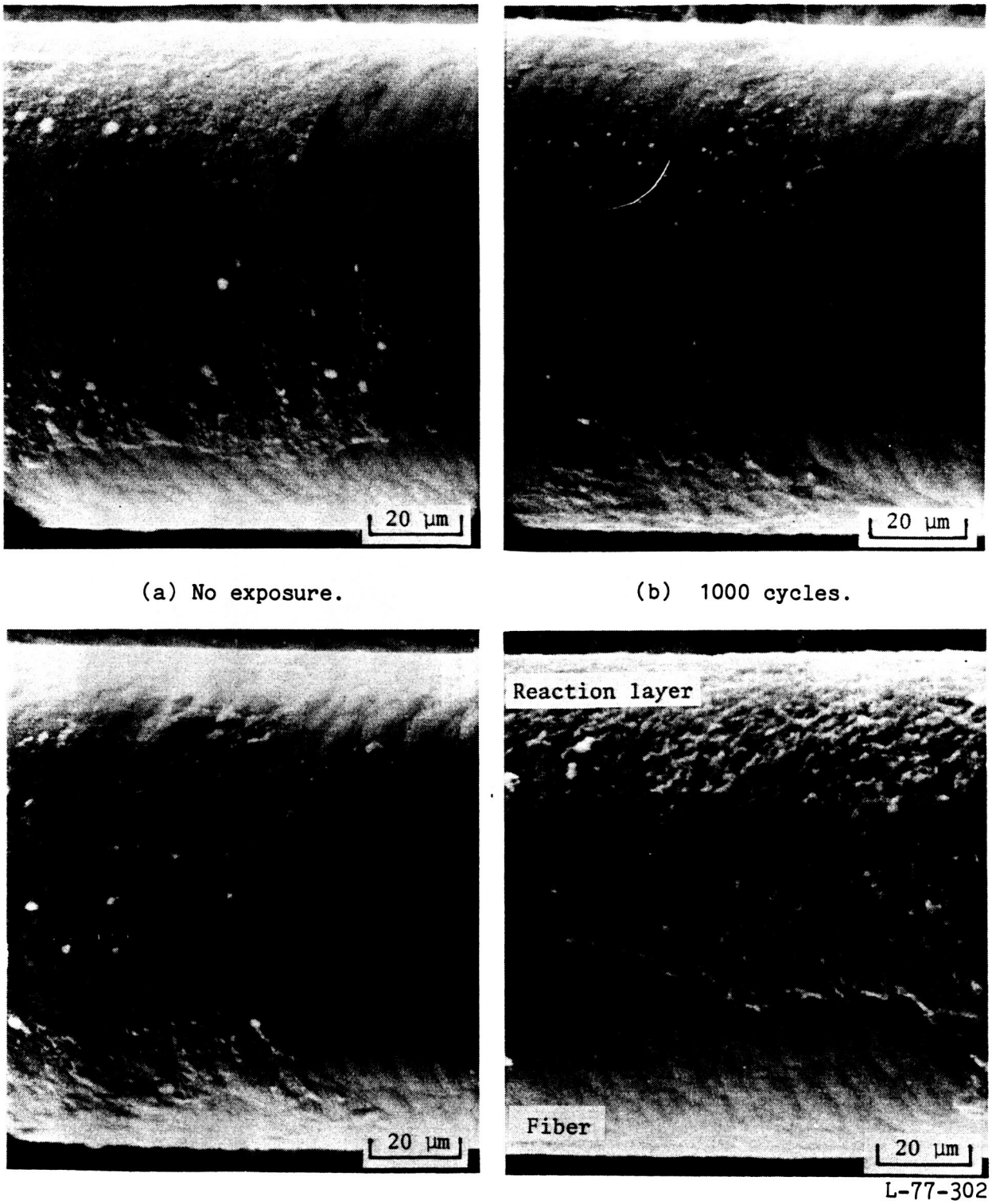

(a) No exposure.

(b) 1000 cycles.

(c) 2057 cycles.

(d) 6000 cycles.

Figure 27.- Surface of fibers from B/Al cyclically exposed between 293 K and 728 K.

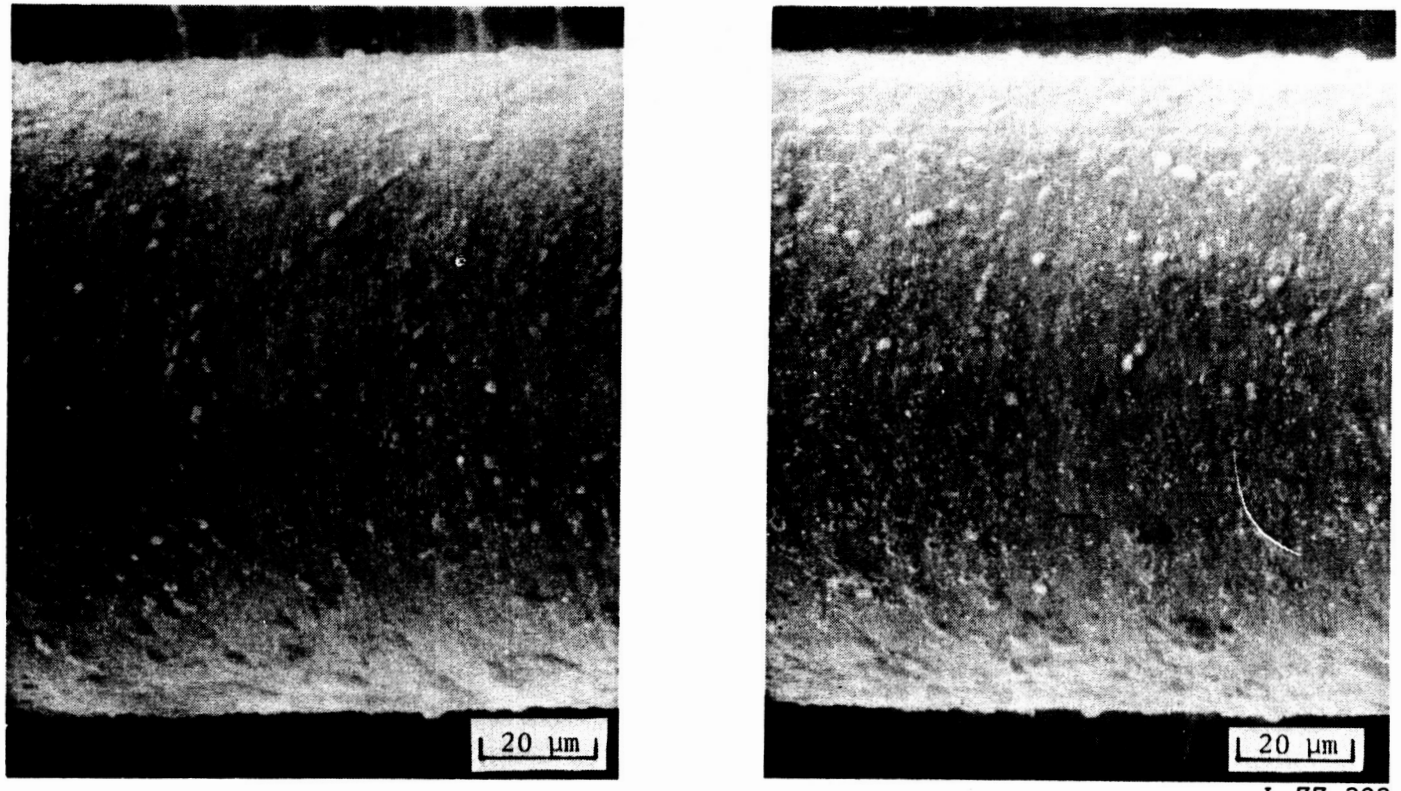

(a) No exposure, unetched.

(b) No exposure, etched.

Figure 28.- Surface of fibers from Bsc/Al cyclically exposed between 293 K and 728 K.

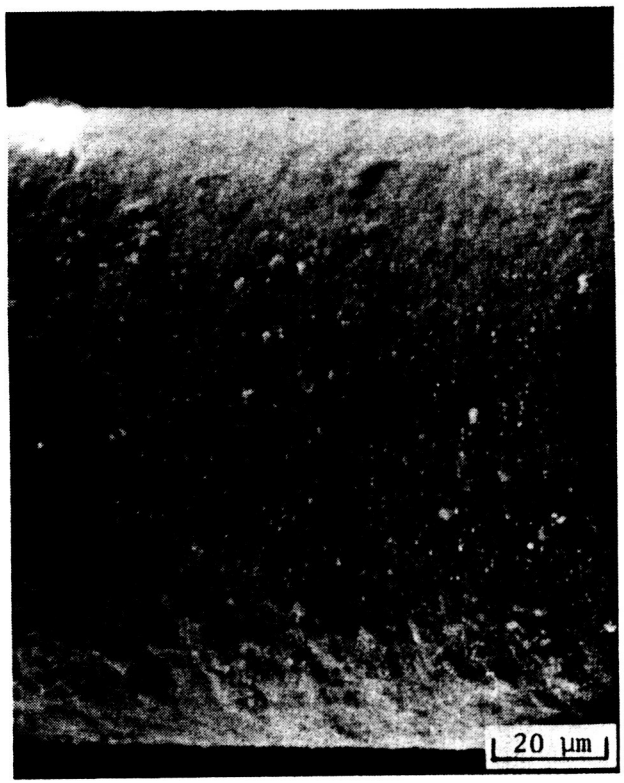

(c) 6000 cycles, unetched.

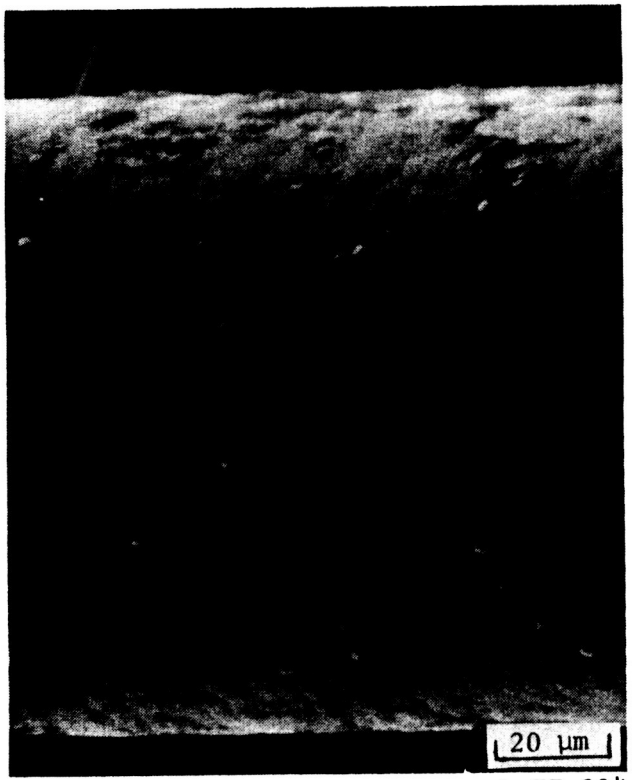

L-77-304

(d) 6000 cycles, etched.

Figure 28.- Concluded.

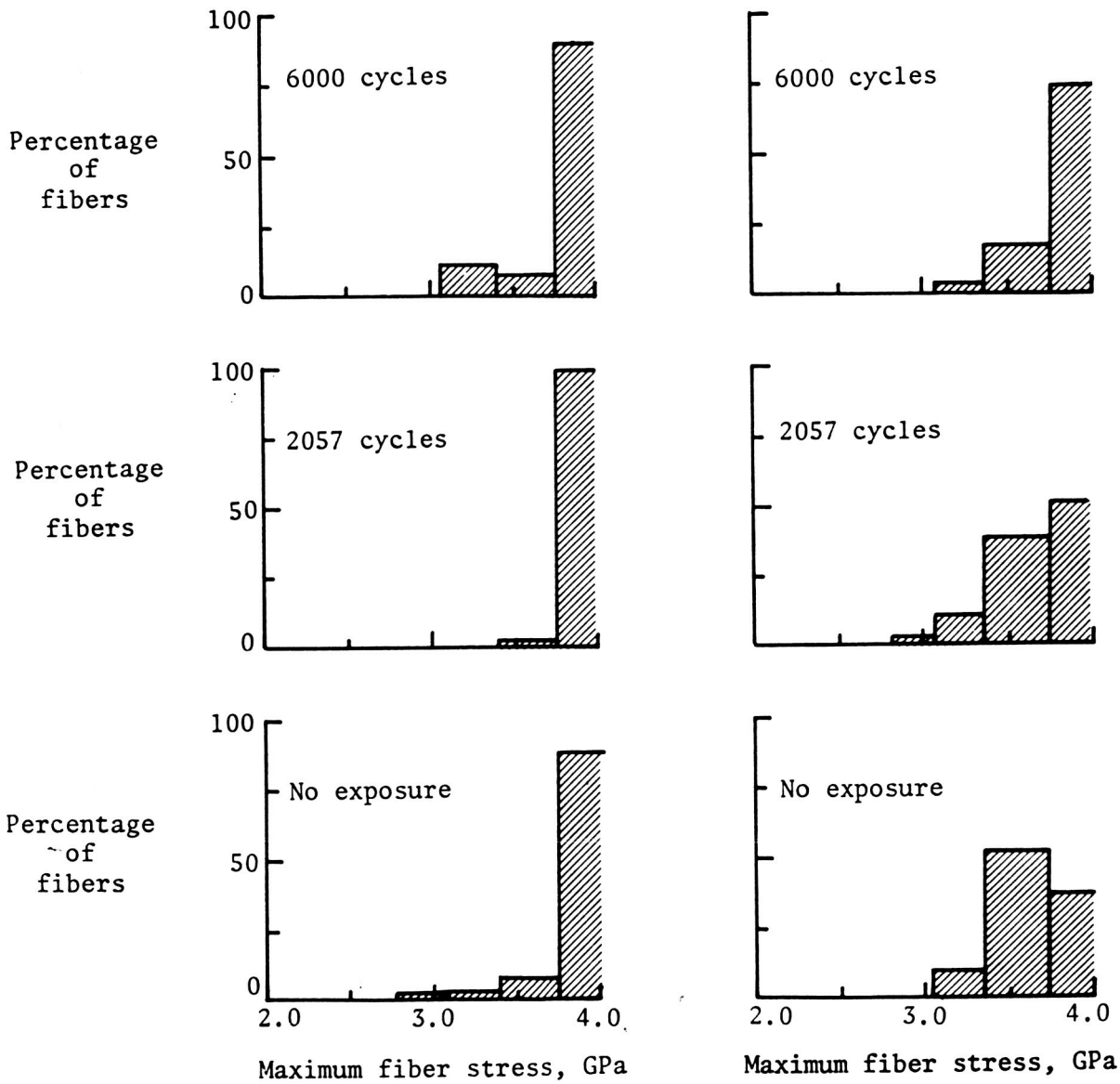

(a) Boron fibers.

(b) Borsic fibers.

Figure 29.- Fiber strength distributions for specimens cyclically exposed between 293 K and 728 K.

1. Report No.	2. Government Accession No.	3. Recipient's Catalog No.
NASA TP-1063		

4. Title and Subtitle	5. Report Date
EFFECTS OF CONTINUOUS AND CYCLIC THERMAL EXPOSURES ON BORON- AND BORSIC-REINFORCED 6061 ALUMINUM COMPOSITES	November 1977
	6. Performing Organization Code

7. Author(s)	8. Performing Organization Report No.
George C. Olsen and Stephen S. Tompkins	L-11722
	10. Work Unit No.
9. Performing Organization Name and Address	506-16-42-01
NASA Langley Research Center Hampton, VA 23665	11. Contract or Grant No.
	13. Type of Report and Period Covered
12. Sponsoring Agency Name and Address	Technical Paper
National Aeronautics and Space Administration Washington, DC 20546	14. Sponsoring Agency Code

15. Supplementary Notes

16. Abstract

Boron-aluminum (B/Al) and Borsic-aluminum (Bsc/Al) composites were continuously exposed at 728 K for up to 240 hours and at 783 K for up to 12 hours and cyclically exposed between 293 K and 728 K for up to 6000 cycles. Tensile strengths were measured and the specimens were metallographically examined. The data suggest that in addition to AlB_2 formation at the fiber/matrix interface, magnesium in the matrix diffused to the reaction layer and formed $(Al,Mg)B_2$. This formation could weaken the matrix and embrittle the reaction layer. Continuous thermal exposure degraded the strength of the B/Al specimens, but the noncumulative fracture mode, indicative of high-strength interfaces, did not change. The strength degradation was attributed to crack initiation in the brittle reaction layer causing stress concentrations on the fibers. Continuous exposure did not alter the strength of the Bsc/Al specimens. Cyclic thermal exposure degraded the strength of both materials, but the strength of the Bsc/Al specimens was degraded to a lesser extent than the B/Al specimens. The cyclic exposure specimens showed transition toward a cumulative fracture mode, characteristic of low interfacial strength. The lower interfacial strengths were attributed to weakened planes caused by reversing stress fields induced by differential thermal expansion. Cyclic exposure degraded the strength of the B/Al specimens more than continuous exposure.

17. Key Words (Suggested by Author(s))	18. Distribution Statement
Metal-matrix composites Thermal degradation Borsic-aluminum Boron-aluminum Thermal fatigue	Unclassified - Unlimited Subject Category 24

19. Security Classif. (of this report)	20. Security Classif. (of this page)	21. No. of Pages	22. Price*
Unclassified	Unclassified	45	$4.00

*For sale by the National Technical Information Service, Springfield, Virginia 22161

NASA-Langley, 1977